

University of Kentucky

UKnowledge

Theses and Dissertations--Electrical and
Computer Engineering

Electrical and Computer Engineering


2018

Stability Analysis and Design of a Tracking Filter for Variable Frequency Applications

Pranav Aramane

University Of Kentucky, aramanepuranav@gmail.com

Author ORCID Identifier:

 <https://orcid.org/0000-0002-5743-5879>

Digital Object Identifier: <https://doi.org/10.13023/ETD.2018.140>

[Right click to open a feedback form in a new tab to let us know how this document benefits you.](#)

Recommended Citation

Aramane, Pranav, "Stability Analysis and Design of a Tracking Filter for Variable Frequency Applications" (2018). *Theses and Dissertations--Electrical and Computer Engineering*. 117.
https://uknowledge.uky.edu/ece_etds/117

This Master's Thesis is brought to you for free and open access by the Electrical and Computer Engineering at UKnowledge. It has been accepted for inclusion in Theses and Dissertations--Electrical and Computer Engineering by an authorized administrator of UKnowledge. For more information, please contact UKnowledge@lsv.uky.edu.

STUDENT AGREEMENT:

I represent that my thesis or dissertation and abstract are my original work. Proper attribution has been given to all outside sources. I understand that I am solely responsible for obtaining any needed copyright permissions. I have obtained needed written permission statement(s) from the owner(s) of each third-party copyrighted matter to be included in my work, allowing electronic distribution (if such use is not permitted by the fair use doctrine) which will be submitted to UKnowledge as Additional File.

I hereby grant to The University of Kentucky and its agents the irrevocable, non-exclusive, and royalty-free license to archive and make accessible my work in whole or in part in all forms of media, now or hereafter known. I agree that the document mentioned above may be made available immediately for worldwide access unless an embargo applies.

I retain all other ownership rights to the copyright of my work. I also retain the right to use in future works (such as articles or books) all or part of my work. I understand that I am free to register the copyright to my work.

REVIEW, APPROVAL AND ACCEPTANCE

The document mentioned above has been reviewed and accepted by the student's advisor, on behalf of the advisory committee, and by the Director of Graduate Studies (DGS), on behalf of the program; we verify that this is the final, approved version of the student's thesis including all changes required by the advisory committee. The undersigned agree to abide by the statements above.

Pranav Aramane, Student

Dr. Aaron Cramer, Major Professor

Dr. Caicheng Lu, Director of Graduate Studies

Stability Analysis and Design of a Tracking Filter for Variable Frequency
Applications

THESIS

A thesis submitted in partial fulfillment of
the requirements for the degree of Master of
Science in Electrical Engineering in the
College of Engineering at the University of
Kentucky

By
Pranav Aramane
Lexington, Kentucky

Director: Dr. Aaron Cramer, Professor of Electrical and Computer Engineering
Lexington, Kentucky 2018

Copyright© Pranav Aramane 2018

ABSTRACT OF THESIS

Stability Analysis and Design of a Tracking Filter for Variable Frequency Applications

The work presented in this thesis is a frequency adaptive tracking filter that can be used in exact tracking of power frequencies and rejection of unwanted harmonics introduced during power disturbances. The power synchronization process includes power converters and other equipment that have many non-linear components that introduce unwanted harmonics. This new design is motivated by the requirement of a filter that can filter all the harmonics and exactly track a rapidly varying fundamental frequency with little time delay and phase error. This thesis analyzes the proposed filter mathematically based on Lyapunov theory and simulations are presented to show the performance of the design in rapid frequency variations.

KEYWORDS: Tracking filter, nonlinear design, harmonics, rapid frequency variation

Author's signature: Pranav Aramane

Date: May 7, 2018

Stability Analysis and Design of a Tracking Filter for Variable Frequency
Applications

By
Pranav Aramane

Director of Thesis: Dr. Aaron Cramer

Director of Graduate Studies: Dr. Caicheng Lu

Date: May 7, 2018

Dedicated to my grandmother
Leela Bhanumurthy Vutukuri

ACKNOWLEDGMENTS

I would like to express my sincere gratitude to my advisor, Dr. Aaron Cramer for his constant guidance and patience. He was always available and helpful, encouraging me throughout my work.

I must express my love and gratitude for my parents without their sacrifices and support I would have not achieved anything. I would also like to express my gratitude to my friends for always being there, especially Ata Arvani, Satya Saurabh Mungamuru for the preliminary proof reading and suggestions. I am also grateful to my mentor, Dr. Srinivasa Lingireddy for his advise and suggestions throughout my studies both in India and US.

TABLE OF CONTENTS

Acknowledgments	iii
Table of Contents	iv
List of Figures	v
List of Tables	vi
Chapter 1 Introduction	1
1.1 Problem - Harmonics	3
1.2 Lyapunov Stability	13
1.3 Second Order Generalized Integrator based Quadrature Signal Generator (SOGI-QSG)	17
1.4 Proposed Filter Design	18
Chapter 2 Mathematical Analysis	20
2.1 Unperturbed Filter Trajectory	20
2.2 Stability of Trajectory System	22
2.3 Properties of Trajectory System	25
2.4 Generalization to Multiple Frequency Inputs	27
2.5 Dynamics of Unperturbed Filter Trajectory	28
Chapter 3 Proposed Design's Simulation Analysis	31
3.1 Selected harmonic source	31
3.2 Filter Parameter Selection	33
3.3 Comparison with standard low pass filter	36
3.4 Variable Frequency Harmonic Distortion Filtering Performance	42
Chapter 4 Conclusion	46
Bibliography	49
Vita	55

LIST OF FIGURES

1.1	Power generation growth in the recent years	1
1.2	Harmonics of a signal	3
1.3	Standard SOGI-QSG	17
2.1	Steady-state normalized magnitude and phase of x_1^* and x_2^* . Normalized frequency is $\omega/\hat{\omega}$	24
2.2	Trade off between bandwidth and settling rate.	26
3.1	Full wave three phase rectifier simulink design	32
3.2	Control parameter (α) value selection based on settling rate and Phase error variation with THD variation.	34
3.3	Harmonically distorted rectifier input voltages v_{ab} and v_{bc}	36
3.4	Comparison of tracking abilities of the proposed filter and a Low pass filter	37
3.5	Phase change and phase error comparison for α & τ at THD = 3% . . .	38
3.6	Output comparison of TF & LPF for α & τ at Settling Rate = 60 rads/s	39
3.7	Phase change and phase error comparison for α & τ at settling rate = 60rads/sec	40
3.8	(a)Filtered Output (b)Error signals of both filters - in variable frequency conditions	43
3.9	Zoomed in plot during the rapid frequency change	43
3.10	Zoomed in plot immediately after rapid frequency change	44
3.11	Zoomed in plot with settled output of TF	44

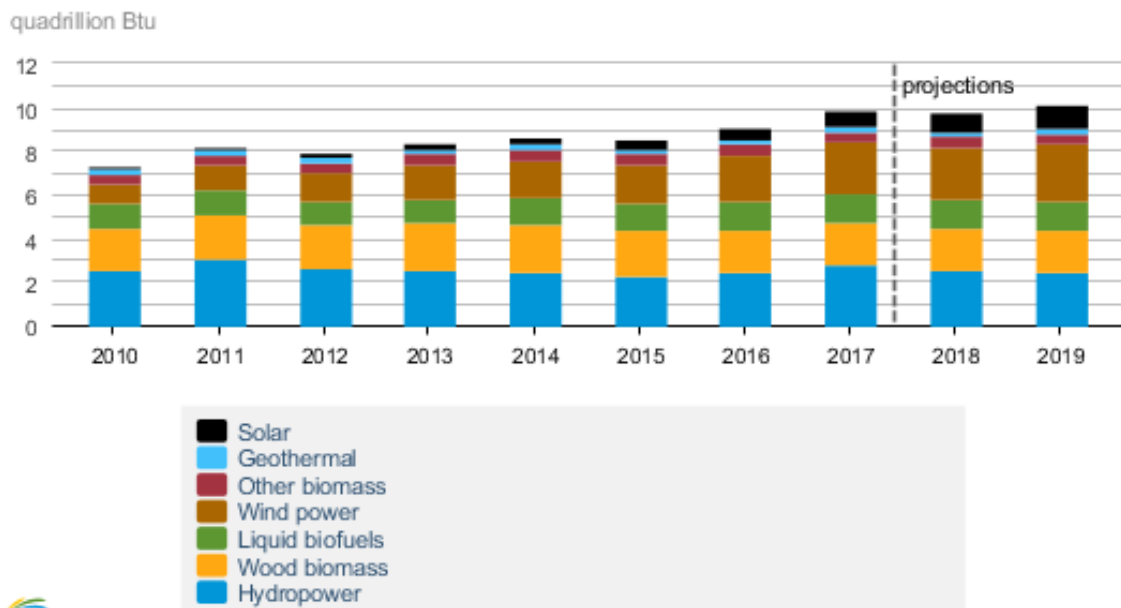
LIST OF TABLES

1.1	Harmonic Distortion Limits According to IEEE STD 519-2014	9
-----	---------------------------------------------------------------------	---

Chapter 1 Introduction

The number of renewable power generation units being integrated into the grid is increasing everyday, with the majority being wind and solar power [1]. This integration had given rise to the concept of Distributed Power Generation Systems (DPGS) where the grid requirement is met by multiple power generation units. The increase in the power generation by various types of sources is shown in the Figure 1.1 from the US Energy Information Administration (EIA) website for 2018 [2]. Major areas of concern in injection of power to the grid from various sources are power control and reliability. These units should be controlled to generate power in a way that they

U.S. renewable energy supply



Source: Short-Term Energy Outlook, February 2018

Note: Hydropower excludes pumped storage generation. Liquid biofuels include ethanol and biodiesel. Other biomass includes municipal waste from biogenic sources, landfill gas, and other non-wood waste.

Figure 1.1: Power generation growth in the recent years

are all synchronized and meet the exact power requirements of the grid;the energy

produced at any given time must be equal to the energy utilized at the particular time.

Controllability of DPGSs is the ability to control the power production (active and reactive), quality of power and the synchronization with the grid at the point of interconnection. To provide a near sinusoidal power at the required frequency and voltage to electrical equipment is power quality (PQ). Various levels of penetration of multiple power generation units coupled with non-linear grid-side loads induce harmonics resulting in significant loss of power quality like voltage unbalance, harmonics, flickers, blackouts etc. Monitoring PQ attributes like rms voltage, harmonic levels, active and reactive component values is now very important due to the increasing grid complexity [3].

This thesis focuses on harmonics, one of the important sources of PQ disturbances. It is imperative that harmful harmonics be identified and filtered to restore the quality of power. A filter that accurately tracks the fundamental frequency and rejects fast varying harmonics has been proposed in this thesis.

This chapter provides a brief a description of the problem, rationale for choosing the point, review of literature pertaining to the topic, and the mathematical background for the proposed filter design. Organization of the thesis is outlined towards the end of the chapter.

1.1 Problem - Harmonics

Basic Definition

Harmonics are components of a signal that are integer multiples of the fundamental frequency of a system. Harmonics are referred by their order which is the integer multiple of the fundamental frequency so, an n^{th} order harmonic has the frequency n times fundamental frequency.

In general power systems around the world operate either at 50 Hz or 60 Hz. In U.S.A it is 60 Hz where, the harmonics of this signal will be 120 Hz, 180 Hz, 240 Hz and so on. Harmonics which are non integer multiples of the fundamental frequency are called inter harmonics.

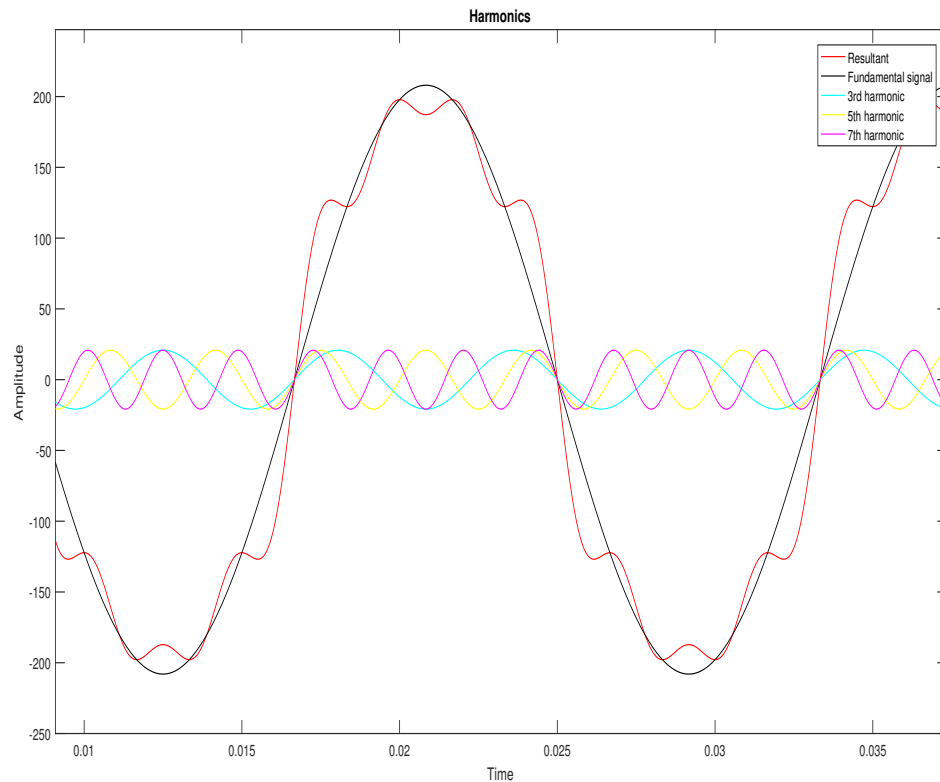


Figure 1.2: Harmonics of a signal

So for the 60 Hz fundamental harmonics with frequency 140 Hz or 190 Hz are

interharmonics. Another type of harmonics are triple- n harmonics which are odd integer multiples of the 3rd harmonic. Harmonics like 9th, 15th, 27th and so on are triple- n harmonics.

In the Figure 1.2 a fundamental waveform and some of its harmonics are shown. It can be observed in this figure how the presence of harmonics distort the fundamental.

Harmonics in power systems is not a recent issue, it was researched by Steinmentz in 1916 in three phase power systems and documented in his published text. This research in harmonics helped in development of new designs for transformers and machines which increased their life and efficiency.

Sources of Harmonics

In the past all the electrical loads were generally linear and due to this the harmonics they generated were negligible. However due to the increase in the use of solid-state devices in almost all the loads for better efficiency and low power consumption most of the loads have become non-linear in nature. In a non-linear device the impedance changes with the applied voltage. Due to this change in impedance the consumed current is non-sinusoidal in nature even though the supplied voltage is sinusoidal in nature. For example, a diode only allows half of the sinusoidal current to pass through. So, non-linear loads produce considerable levels of harmonics that distort the power signals.

On the power generation side, in addition to the generator the increasing use of non-linear devices in power control systems lead to a high harmonic pollution [4]

1. *Power converters and Interconnection devices*: They produce current harmonics due to the non-linear switching operation. This harmonic pollution has been significantly reduced by replacing the SCR power inverters by IGBT inverter designs.

2. *Synchronous Generators*: Generators produce harmonics on the basis of their coil design - its non-linearity, grounding and so on.

Impact of distributed generation (DG) penetration on power harmonics was studied in [5], with a particular reference to PV DG system. An overview of the various control structures is provided in [6] for DPGS based on fuel cells, PV, and wind turbines.

While on the load side most devices in the present are integrated with non-linear devices. For example:

1. Personal computers
2. Air conditioners
3. Uninterrupted power supplies [7] inject harmonics into the grid.

Almost all of these devices use Solid State Power Switching Supplies to convert incoming AC to DC, which have non-linear operation characteristics. In the case of variable frequency drives, AC to DC converters are either diode or SCR-type which produce a great magnitude of harmonics. The research paper [8] shows the amount of harmonic distortion produced by some of the day to day appliances when compared to a linear load.

In general, the grid frequency varies randomly in a narrow range of less than ± 0.5 Hz . As the behavior of harmonics is dependent on fundamental frequency; they may vary in frequency, phase and magnitude along with the fundamental.

1. *Variable Frequency Drives (VFDs)*: VFDs exhibit sudden breaking and starting operations, which produce time varying current amplitudes, causing time varying power harmonics.
2. *Cycloconverters*: They convert the input 60 Hz power to adjustable variable frequency output is used with a VFD for applications like mining. These con-

verters differ from general converters as they do not have a dc link in the design and rely on switching the phase of the input to give the desired output frequency. When the converter is used to ramp up the speed of the drive the frequency of the harmonics and inter-harmonics vary. This is presented in the research paper [9] where the analysis of the harmonic components including inter-harmonics is done for various speed ramp up operations.

3. *Electric Arc Furnace (EAF)*: Arc furnaces are used for melting in metallurgy industry. They operate by producing high temperatures by electric arcs. During the different stages of metal shaping and refinement the arc characteristics vary drastically and cause harmonics. [10]

Effects of Harmonics

Harmonics if injected into the grid at the point of interconnection, will cause instability in the power system. They will affect the equipment used in the power distribution network and also the loads connected to it. Harmonics are not transient events which occur for short duration, for example, few seconds or less. They are steady state or quasi-steady state events which cause continuous distortion in voltage and current.

Some of the major negative impacts of harmonics are listed below [11] [12] [13] [14]:

1. *Electric Lines*: Damage because of conductor overheating due to skin effect. Insulator degradation caused due to dielectric breakdown. Transmission losses due to corona effect and losses transversal losses.
2. *Capacitors*: Decrease in life and efficiency due to dielectric failure and heating. Failure from reactive power overload. Capacitors in transmission lines are used to improve power factor, these enable resonant conditions for harmonics which causes large current and voltages in the lines.
3. *False operation of fuses and circuit breakers*

4. Transformers: Damage due to stray flux losses and copper losses. Power loss due to short-circuit losses and hysteresis losses.
5. Voltage Regulators: Harmonics effect the timing due to increase of multiple zero crossings in the current waveform in turn destabilizing the generator.
6. Electronic Equipment: Multiple zero crossing caused due to harmonic distortion in the semiconductor elements will cause changes in the switching times of the devices. The inter-harmonics effect devices with cathode ray tubes and cause random variations in the image size.
7. Machinery: Non-sinusoidal currents cause over heating and in rotating parts pulsating torques and noise.
8. Telecommunication: Harmonics in power lines produce varying electric and magnetic fields which effect the communication systems due to proximity.

These negative effects of harmonics will be further increased due to resonance where the harmonic frequency is close to the system's natural frequency [15]. The damage due to harmonics can be short term in cases like malfunctioning of relays and breakers but in cases of over heating of lines, transformer damage etc they affect the life span of equipment. In both the scenarios of short and long term damage due to the demand for reliable power and complexity of the grid the economic losses to the generator, distributor as well as the consumer is very high.

Estimation and Measurement

To avoid the negative effects and control the power quality it is imperative to estimate and measure harmonic distortion so as to accurately eliminate their presence in the power system.

Harmonic content in a system can be estimated by several methods and new methods are continuously being developed and improved for this purpose.

Literature review of recently published estimation techniques:

1. A paper that proposes Hilbert transform signal processing techniques coupled with matrix calculations where characteristics of signals are obtained and analyzed to estimate real time accurate harmonic estimations was published in [16].
2. A frequency shifting and filtering algorithm is described in this publication [17] where an iterative smoothing filter is used to eliminate the distortions after a frequency shift of the original signal is done and the error between the original and frequency shifted signal provides the harmonic estimation.
3. A frequency domain analysis of 3-phase system signal is done in the proposed algorithm [18] where the Fourier coefficients are interpolated after using Clarke's transform to convert the signal to a harmonic exponential signal. This gives a rapid analysis of frequency, phase and amplitude of the fundamental gives an estimate of the harmonic distortion.

Mathematically the effect of harmonics in a network can be measured by the the different indices defined in IEC 61000-4-7. This standard defines methods to measure the overall harmonic/inter-harmonic voltages and currents in power systems. Several relationships derived from Fourier series are defined here. The most important being Total Harmonic Distortion (THD)

THD is defined as the ratio of sum of all the harmonic components to the value of the fundamental frequency.

$$THD = \frac{V_{harmonic}}{V_{fundamental}} * 100\%$$

There are many existing standards for harmonic control like International Electrotechnical Committee (IEC), IEEE & IET. There is ongoing effort to coordinate and modify IEEE standards on harmonic control, published in 1992 with IEC [19, Page

4]. According to these standards the maximum permissible harmonic distortion percentage varies with the voltage level. Allowed limits are [19, Sec 5.1]:

Table 1.1: Harmonic Distortion Limits According to IEEE STD 519-2014

Bus Voltage V at PCC	Individual Harmonic (%)	Total Harmonic Distortion THD (%)
$V \leq 1.0$ kV	5.0	8.0
1 kV $< V \leq 69$ kV	3.0	5.0
69 kV $< V \leq 161$ kV	1.5	2.5
161 kV $< V$	1.0	1.5

Mitigation Techniques

Various hardware control structures and control strategies for restoring the quality of power of DPGS are described in [6, 20]. These references also provide an overview of various grid synchronization algorithms, along with a discussion on their influence and role in the control of DPGS on normal and faulty grid conditions.

Most of the traditional techniques for harmonic removal in power are designed for steady state. However, due to the time varying conditions it is imperative to analyze and remove harmonics in transient state in order to achieve better control of the system [21].

Harmonic filtering techniques can be broadly classified into passive, active or a combination of passive and active.

Passive filters use capacitors, reactors and resistors in combinations of RC, RL, LC or RLC. They are generally tuned to remove certain specific frequencies. This requires great amount of study to determine the quality of harmonics to exactly tune the filter. Due to this limitation, they are not very effective in the cases of dynamic harmonic frequencies and variable loads. Another disadvantage of passive filtering is that the

attenuation efficiency is very low in the cases of higher order harmonic frequencies. However they also induce more distortions by injecting additional harmonics due to their nonlinearity. They are very economical due to which they are widely used in the industry.

Active Harmonic Filters (AHFs) are used to mitigate the distortion by measuring the harmonics and compensating for the distortion caused by them. In AHFs there are two parts - one for measuring the parameters of harmonics the other for controlling the distortion [22]. The control strategy in AHFs can be implemented either in time or frequency domain. Frequency domain control is the most commonly used strategy. In this method Fourier Transform and its variations like Fast Fourier Transform (FFT), Discrete Fourier Transform (DFT) are implemented. The basic principle of the frequency domain control method is to isolate the fundamental from harmonics by performing an inverse Fourier Transform and then calculating the reference signal in order to compensate for the distortion. This method is not practically viable due to the time delay introduced by it for variable load applications. Advanced Active Filtering techniques use signal processing methods to estimate and control the distortion in nonlinear networks with variable signal parameters. Some of the most commonly used techniques are Fuzzy Logic, Kalman Filter, PLL's [23].

Tracking

In the active filtering method, the signal measurement component tracks the required signal either fundamental or a particular harmonic. This is an effective way to get a high efficiency compensation signal.

Tracking sinusoids in noise is a common procedure, it is widely used in communications, radar, power systems line synchronization and spectral analysis applications.

For example, Kalman filter and its variants are used in Radar to remove noise from tracking measurements and to get a more accurate estimated position of the

target [24]. In communications, tracking filters are used in information transmission to deal with uncertain measurements caused by quantization error [25]. In sound engineering they are used for auditory scene analysis to extract the main or required stream of audio from multiple sound streams [26]. Traditionally to track sinusoids with varying parameters methods like FIR filters combined with Least Mean Square (LMS) algorithm, Phase-Lock Loops (PLL) [27]- [28] and adaptive constrained Infinite Impulse Response (IIR) structures [29] are used.

In a three phase system frequency is an important quality parameter. To maintain stability it is important for fast and accurate estimation of its time varying frequency when it is distorted by harmonics. Taking into consideration all the harmonics produced in a three phase system, the most distortion is caused by the 3rd harmonic of the fundamental. The third harmonic unlike the other harmonic signals is identical in all the three phases which makes its sum in the neutral not equal to zero. This causes it to add up in the neutral and overload the system. This property is also applicable to all the triple- n harmonics - all the odd multiples of the 3rd harmonic (9th, 15th etc.) [30]. It is important to identify such harmonics generated in the system and eliminate them to improve the power quality.

To meet these requirements a design for a filter to accurately track the fundamental and reject the fast varying harmonics in the power signal is proposed in this thesis. Working on a method to detect line-to-ground faults in high resistance ground networks, Rodriguez-Valdez and Kerkman [31] proposed a non-linear tracking filter to ensure adequate tracking of the current and voltage signatures. This non-linear tracking filter forms the basis for the thesis.

Organization of the thesis

The Thesis is organized as four chapters.

The first chapter gives a basic overview of the problem with the negative impacts due to it and background information of the existing solutions. It also covers some basic mathematical background required to understand the analysis and the proposal of the design.

Chapter 2 presents the mathematical analysis of the tracking filter by first defining its unperturbed trajectory then analyzing the trajectory's stability and properties. This analysis is then generalized for inputs with noise. The design's trajectory is then assessed for input-to-state stability. The parameters for control gain for the proposed filter are selected based on the settling rate, phase error and THD values required.

The performance of the Filter is then shown in Chapter 3 where it is compared with a standard low pass filter and the QSG-SOGI filter.

The conclusion and ideas for further development on the proposed design and applications are discussed in Chapter 4.

1.2 Lyapunov Stability

Lyapunov stability theory is a standard tool which plays a very important role in system analysis and control design of nonlinear systems. This theory is an effective way to analyze the stability of non-linear differential equations with solutions that are difficult to obtain.

A general nonlinear system can be defined as

$$\dot{x}(t) = f(t, x(t)) \quad (1.1)$$

where $x : \mathfrak{R} \rightarrow \mathfrak{R}^n$ and $f : \mathfrak{R} \times \mathfrak{R}^n \rightarrow \mathfrak{R}^n$ are functions and if $x(t) = (x_1(t), \dots, x_n(t))$ where all the component functions are real-valued functions on \mathfrak{R} then

$$\dot{x}(t) = (\dot{x}_1(t), \dots, \dot{x}_n(t)).$$

In some cases we will be considering the autonomous case

$$\dot{x}(t) = f(x(t)) \quad (1.2)$$

where $f : \mathfrak{R}^n \rightarrow \mathfrak{R}^n$.

In this system when at a time t_0 if $x(t_0) = x_0$ such that $f(x_0) = 0$ that the point x_0 is an equilibrium point of the system. Lyapunov theory is used to define the stability of these equilibrium points [32].

Definition 1.2.1 *A solution $x(t)$ is stable if for every $\varepsilon > 0$ there exists $\delta > 0$ such that if $\|x_0 - \bar{x}_0\| < \delta$ then $\|x(t) - \bar{x}(t)\| < \varepsilon$ for every $t \geq t_0$, where $\bar{x}(t)$ is the solution to*

$$\dot{\bar{x}}(t) = f(t, \bar{x}(t))$$

with $\bar{x}(t_0) = \bar{x}_0$.

Lyapunov theory gives the flexibility to determine the stability without the solution for the differential equations. It does not require a characterization of the solutions to determine stability.

For this purpose we use a function that satisfies the condition of being zero at equilibrium but positive definite everywhere else and as $x \rightarrow$ equilibrium $V(x)$ decreases, basically $V(x)$ is such that $\Delta V(x) < 0$.

Let $V : D \rightarrow \mathfrak{R}^n$ be a continuously differentiable function defined in a domain $D \subset \mathfrak{R}^n$ that contains origin. The derivative of V along trajectories of (1.1), denoted by $\dot{V}(x)$, is given by

$$\dot{V} = \sum_{i=1}^n \frac{\partial V}{\partial x_i} f_i(t, x) = \frac{\partial V}{\partial x} f(x)$$

If $\dot{V}(x)$ is negative, V will decrease along the trajectory of (1.1) passing through x . A function $V(x)$ is positive definite if $V(0) = 0$ and $V(x) \geq 0$ for $x \neq 0$. A function $V(x)$ is negative definite or negative semidefinite if $-V(x)$ is positive definite or positive semidefinite, respectively.

Lyapunov's stability theorem states that the origin is stable if, in a domain D that contains the origin, there is a continuously differentiable positive definite function $V(x)$ so that $\dot{V}(x)$ is negative semidefinite, and it is asymptotically stable if $\dot{V}(x)$ is a negative definite. When the condition for stability is satisfied, the function V is called a Lyapunov function [32, Theorem 4.1, Page 117]

In this thesis the stability of the proposed design is calculated considering the following general form of the non linear system

$$\dot{x}(t) = A(t)x + bu(t) \tag{1.3}$$

For this system let us consider the Lyapunov function $V(x) = x^T P x$ as the Lyapunov function where P is a real symmetric positive definite matrix. Calculating the

derivative of $V(x)$

$$\begin{aligned}\dot{V}(x) &= x^T P \dot{x} + (\dot{x})^T P x \\ \dot{V}(x) &= x^T P [Ax + bu(t)] + [x^T A^T + u(t)b^T] P x \\ \dot{V}(x) &= x^T [PA + A^T P]x + 2x^T Pbu(t) \\ \text{Let } [PA + A^T P] &= -Q \\ \implies \dot{V}(x) &= -x^T Qx + 2x^T Pbu(t)\end{aligned}$$

Here the value of b is indefinite as it varies from one system to another. By the Lyapunov theory if $\dot{V} \leq 0$ then the system is asymptotically stable. So we calculate the left hand terms value and determine if the \dot{V} of the proposed filter is negative.

Lyapunov's theorem can be applied without solving the differential equation (1.1). There is no method for finding Lyapunov functions. In some cases, there are natural Lyapunov functions for systems of energy functions in electrical or mechanical systems. In all other cases, it is trial and error.

The Lyapunov function even if is proven to be continuous does not guarantee Global Asymptotic Stability (GAS). So, to further prove the robustness of the proposed design we analyze it for input-to-state stability [32, Page 174].

Definition 1.2.2 *A system is said to be input-to-state stable if there exists a $K\mathcal{L}$ function β and a class K function γ such that for any initial state $x(t_0)$ and any bounded input $u(t)$, the solution $x(t)$ exists for all $t \geq t_0$ and satisfies*

$$\|x(t)\| \leq \beta(\|x(t_0)\|, t - t_0) + \gamma(\sup_{t_0 \leq r \leq t} \|u(r)\|)$$

Here β and γ are Comparison Functions [32, Page 144]. These functions are calculated [32, Theorem 4.10, Theorem 4.19] based on the differentiability of the Lyapunov

function V . If $V(x)$ is continuously differentiable function such that

$$\theta_1 \|x\|^\delta \leq V(t, x) \leq \theta_2 \|x\|^\delta$$

$$\text{and } \dot{V} \leq -\theta_3 \|x\|^\delta \quad \forall \quad \|x\| \geq \rho \|u\| > 0$$

$$\text{then } \beta = \left(\frac{\theta_2}{\theta_1}\right)^{\frac{1}{\delta}} \|x(t_0)\| e^{-(\theta_3/\theta_2\delta)(t-t_0)} \quad \text{and} \quad \gamma = \theta_1^{-1} * \theta_2 * \rho$$

1.3 Second Order Generalized Integrator based Quadrature Signal Generator (SOGI-QSG)

A quadrature signal generator is a widely used tool in motion control and signal processing. some of its important applications in power systems are single and three phase grid synchronization and real time power measurement in single phase systems [33]. In fig 1.3 a standard SOGI-QSG is shown as a signal flow graph.

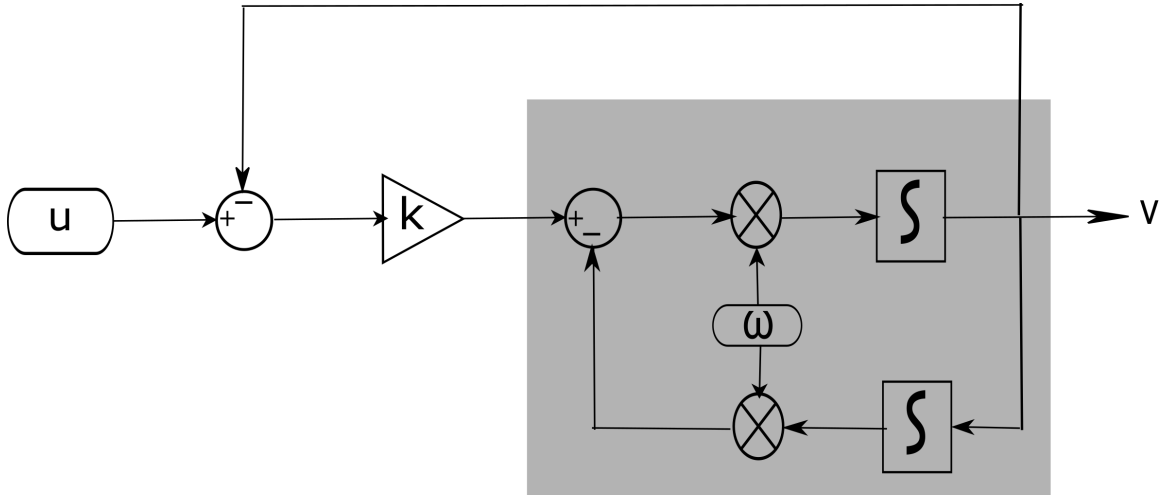


Figure 1.3: Standard SOGI-QSG

A SOGI based QSG is most widely used because of its simplicity. This filter is used in many applications like real time estimation of voltage components of an unbalanced single phase grid [34], extraction of orthogonal fundamental power wave forms [35] in combination with Kalman filters to analyze the PQ etc. SOGI-QSG has the advantage over other QSG's of providing a notch filter effect in the output.

It is used in combination of Phase Locked Loops (PLL) to filter harmonics during grid frequency fluctuations due to its fast dynamic response. These papers study different applications of the SOGI-QSG for various harmonic mitigation implementations involving PLLs [36] [37] [38].

Different Fourier transform techniques with SOGI-PLL are used in [36] to compen-

sate harmonics in a three-phase PV inverter. The paper [37] analyses the advantages and disadvantages of using a Frequency Fixed SOGI-PLL in combination of compensation elements to filter harmonics. SOGI in [38] is used in a Differentiator Decouple Filter to filter harmonic disturbances in the output of Synchronous Reference Frame-PLL.

This makes the SOGI-QSG ideal to compare the proposed design in this thesis in variable frequency conditions.

1.4 Proposed Filter Design

The tracking filter system proposed in [31] is improved and analyzed in this paper, rather than focusing in varying parameters, it is assumed that the frequency is known; and then, the focus shifts towards having an implementation (realization) that allows for improved tracking in transient and in steady-state.

The main focus of the design is its use in variable frequency applications. Many existing techniques like Short Time Fourier Transform, Least Mean Square approach, Kalman filtering cannot rapidly track frequency/amplitude/phase time varying harmonics.

The proposed filter is mathematically analyzed and proven to be stable, its tracking ability and settling rate are also established. Matlab and Simulink simulations are then used to show the filter's performance as opposed to a low pass filter. It is also compared with the novel SOGI-QSG filter in terms of tracking and is proved to perform better during rapid frequency fluctuations in the fundamental frequency that can be generally observed in renewable energy integrated power grids.

The proposed tracking filter in this paper is designed to have higher frequency dependency than the SOGI-QSG. The two mentioned filters behave similarly when the fundamental frequency of the signal remains constant but the proposed filter gives a significantly better tracking performance under variable frequency conditions.

Mathematical Representation

The improved tracking filter design is mathematically represented in terms of differential equations below.

$$\dot{x}_1 = -\alpha\hat{\omega}(t)x_1 - \hat{\omega}(t)x_2 + \alpha\hat{\omega}(t)u(t) \quad (1.4)$$

$$\dot{x}_2 = \hat{\omega}(t)x_1 \quad (1.5)$$

where $u(\cdot)$ is the input signal, $\alpha > 0$ is control gain constant, $\hat{\omega}(\cdot) \in [\hat{\omega}_{min}, \hat{\omega}_{max}]$ is the (externally) estimated frequency of the signal to be tracked, and x_1 and x_2 are the state variables associated with the filter. At some initial time t_0 , the state variables have initial values $x_1(t_0) = x_{10}$ and $x_2(t_0) = x_{20}$. It is assumed throughout that $\hat{\omega}_{min} > 0$.

The filter can be expressed more compactly as

$$\dot{\mathbf{x}} = \underbrace{\begin{bmatrix} -\alpha\hat{\omega}(t) & -\hat{\omega}(t) \\ \hat{\omega}(t) & 0 \end{bmatrix}}_{\mathbf{A}(t)} \mathbf{x} + \underbrace{\begin{bmatrix} \alpha\hat{\omega}(t) \\ 0 \end{bmatrix}}_{\mathbf{b}} u(t) \quad (1.6)$$

where $\mathbf{x} = [x_1 \ x_2]^T$ and $\mathbf{x}(t_0) = \mathbf{x}_0$.

Chapter 2 Mathematical Analysis

The unperturbed input to the filter can be modeled as a sinusoidal signal with time-varying amplitude and frequency:

$$u^*(t) = M(t) \cos \theta \quad (2.1)$$

$$\dot{\theta} = \omega(t) \quad (2.2)$$

where $\theta(t_0) = \theta_0$. The actual input to the filter may be perturbed by additive noise $v(t)$ such that

$$u(t) = u^*(t) + v(t). \quad (2.3)$$

It is assumed throughout that $\hat{\omega}(\cdot)$, $M(\cdot)$, $\omega(\cdot)$, and $v(\cdot)$ are piecewise continuous, ensuring the existence and uniqueness of the solution of each initial value problem described within.

2.1 Unperturbed Filter Trajectory

If the filter described above is not perturbed by noise ($v(t) = 0$ and $u(t) = u^*(t)$), then its trajectory can be analyzed as follows. Let

$$x_1^* = A_1 \cos \theta + B_1 \sin \theta \quad (2.4)$$

$$x_2^* = A_2 \cos \theta + B_2 \sin \theta \quad (2.5)$$

and $\mathbf{x}^* = [x_1^* \ x_2^*]^T$. The coefficients A_1 , B_1 , A_2 , and B_2 evolve according to

$$\dot{\tilde{\mathbf{x}}} = \underbrace{\begin{bmatrix} -\alpha\hat{\omega}(t) & -\omega(t) & -\hat{\omega}(t) & 0 \\ \omega(t) & -\alpha\hat{\omega}(t) & 0 & -\hat{\omega}(t) \\ \hat{\omega}(t) & 0 & 0 & -\omega(t) \\ 0 & \hat{\omega}(t) & \omega(t) & 0 \end{bmatrix}}_{\tilde{\mathbf{A}}(t)} \tilde{\mathbf{x}} + \underbrace{\begin{bmatrix} \alpha\hat{\omega}(t) \\ 0 \\ 0 \\ 0 \end{bmatrix}}_{\tilde{\mathbf{b}}} \tilde{u}(t) \quad (2.6)$$

where $\tilde{\mathbf{x}} = [A_1 \ B_1 \ A_2 \ B_2]^T$ and $\tilde{u}(t) = M(t)$. Also, let $\tilde{\mathbf{x}}(t_0) = \tilde{\mathbf{x}}_0$ be a solution to

$$\begin{bmatrix} \cos \theta_0 & \sin \theta_0 & 0 & 0 \\ 0 & 0 & \cos \theta_0 & \sin \theta_0 \end{bmatrix} \tilde{\mathbf{x}}_0 = \mathbf{x}_0. \quad (2.7)$$

It can be seen that the $\mathbf{x}^*(t_0) = \mathbf{x}_0^* = \mathbf{x}_0$. Furthermore,

$$\begin{aligned} \dot{x}_1^* &= \dot{A}_1 \cos \theta - \omega(t)A_1 \sin \theta + \dot{B}_1 \sin \theta + \omega(t)B_1 \cos \theta \\ &= (-\alpha\hat{\omega}(t)A_1 - \omega(t)B_1 - \hat{\omega}(t)A_2 + \alpha\hat{\omega}(t)M(t)) \cos \theta \\ &\quad - \omega(t)A_1 \sin \theta + (\omega(t)A_1 - \alpha\hat{\omega}(t)B_1 - \hat{\omega}(t)B_2) \sin \theta \\ &\quad + \omega(t)B_1 \cos \theta \\ &= -\alpha\hat{\omega}(t)x_1^* - \hat{\omega}(t)x_2^* + \alpha\hat{\omega}(t)u^*(t) \end{aligned} \quad (2.8)$$

$$\begin{aligned} \dot{x}_2^* &= \dot{A}_2 \cos \theta - \omega(t)A_2 \sin \theta + \dot{B}_2 \sin \theta + \omega(t)B_2 \cos \theta \\ &= (\hat{\omega}(t)A_1 - \omega(t)B_2) \cos \theta - \omega(t)A_2 \sin \theta \\ &\quad + (\hat{\omega}(t)B_1 + \omega(t)A_2) \sin \theta + \omega(t)B_2 \cos \theta \\ &= \hat{\omega}(t)x_1^*. \end{aligned} \quad (2.9)$$

Thus, the unperturbed trajectory of (1.6) is described by (2.4) and (2.5) where the coefficients evolve according to (2.6).

2.2 Stability of Trajectory System

The stability of the trajectory system in (2.6) can be understood by consideration of the following Lyapunov function:

$$\tilde{V}(\tilde{\mathbf{x}}) = \underbrace{\tilde{\mathbf{x}}^T \begin{bmatrix} 1 & 0 & \tilde{k} & 0 \\ 0 & 1 & 0 & \tilde{k} \\ \tilde{k} & 0 & 1 & 0 \\ 0 & \tilde{k} & 0 & 1 \end{bmatrix}}_{\tilde{\mathbf{P}}} \tilde{\mathbf{x}} \quad (2.10)$$

where

$$0 < \tilde{k} < \frac{4\alpha}{4 + \alpha^2} \in (0, 1] \quad (2.11)$$

for $\alpha > 0$. The positive definiteness of symmetric $\tilde{\mathbf{P}}$ can be assessed through its eigenvalues, which are $1 \pm \tilde{k}$, each with multiplicity two. Each of these is positive for $|\tilde{k}| < 1$. Therefore, the eigenvalues of symmetric $\tilde{\mathbf{P}}$ are positive, $\tilde{\mathbf{P}}$ is a positive-definite matrix, and $\tilde{V}(\cdot)$ is a positive-definite function. Furthermore,

$$(1 - \tilde{k})\|\tilde{\mathbf{x}}\|^2 \leq \tilde{V}(\tilde{\mathbf{x}}) \leq (1 + \tilde{k})\|\tilde{\mathbf{x}}\|^2. \quad (2.12)$$

Let

$$\begin{aligned} \tilde{\mathbf{Q}}(t) &= -(\tilde{\mathbf{A}}^T(t)\tilde{\mathbf{P}} + \tilde{\mathbf{P}}\tilde{\mathbf{A}}(t)) \\ &= \begin{bmatrix} 2(\alpha - \tilde{k})\hat{\omega}(t) & 0 & \alpha\tilde{k}\hat{\omega}(t) & 0 \\ 0 & 2(\alpha - \tilde{k})\hat{\omega}(t) & 0 & \alpha\tilde{k}\hat{\omega}(t) \\ \alpha\tilde{k}\hat{\omega}(t) & 0 & 2\tilde{k}\hat{\omega}(t) & 0 \\ 0 & \alpha\tilde{k}\hat{\omega}(t) & 0 & 2\tilde{k}\hat{\omega}(t) \end{bmatrix}. \end{aligned} \quad (2.13)$$

The positive definiteness of symmetric $\tilde{\mathbf{Q}}(t)$ can be assessed through its eigenvalues, which are $(\alpha \pm \sqrt{\alpha^2 + 4\tilde{k}^2 + \alpha^2\tilde{k}^2 - 4\alpha\tilde{k}})\hat{\omega}(t)$, each with multiplicity two. Each of these is positive for $4\tilde{k}^2 + \alpha^2\tilde{k}^2 - 4\alpha\tilde{k} < 0$. Suppose $\exists \hat{\omega} \in [\hat{\omega}_{min}, \hat{\omega}_{max}]$ such that

$4\tilde{k}^2 + \alpha^2\tilde{k}^2 - 4\alpha\tilde{k} \geq 0$. Then,

$$(4\tilde{k} + \alpha^2\tilde{k} - 4\alpha)\tilde{k} \geq 0 \quad (2.14)$$

$$4\tilde{k} + \alpha^2\tilde{k} - 4\alpha \geq 0 \quad (2.15)$$

$$4\tilde{k} + \alpha^2\tilde{k} \geq 4\alpha \quad (2.16)$$

$$(4 + \alpha^2)\tilde{k} \geq 4\alpha \quad (2.17)$$

$$\tilde{k} \geq \frac{4\alpha}{4 + \alpha^2} \quad (2.18)$$

which is impossible over $[\hat{\omega}_{min}, \hat{\omega}_{max}]$ by (2.11). Therefore, the eigenvalues of symmetric $\tilde{\mathbf{Q}}(t)$ are positive, and $\tilde{\mathbf{Q}}(t)$ is a positive-definite matrix. Further, let

$$\tilde{\lambda} = (\alpha - \sqrt{\alpha^2 + 4\tilde{k}^2 + \alpha^2\tilde{k}^2 - 4\alpha\tilde{k}})\hat{\omega}_{min}. \quad (2.19)$$

From above, $\tilde{\lambda} > 0$ is a lower bound on the eigenvalues of $\tilde{\mathbf{Q}}(t)$ and

$$-\tilde{\mathbf{x}}^T \tilde{\mathbf{Q}}(t) \tilde{\mathbf{x}} \leq -\tilde{\lambda} \|\tilde{\mathbf{x}}\|^2. \quad (2.20)$$

The time derivative of the Lyapunov function is

$$\begin{aligned} \dot{V} &= (\tilde{\mathbf{x}}^T \tilde{\mathbf{A}}^T(t) + \tilde{u}(t) \tilde{\mathbf{b}}^T) \tilde{\mathbf{P}} \tilde{\mathbf{x}} + \tilde{\mathbf{x}}^T \tilde{\mathbf{P}} (\tilde{\mathbf{A}}(t) \tilde{\mathbf{x}} + \tilde{\mathbf{b}} \tilde{u}(t)) \\ &= -\tilde{\mathbf{x}}^T \tilde{\mathbf{Q}}(t) \tilde{\mathbf{x}} + 2\tilde{\mathbf{x}}^T \tilde{\mathbf{P}} \tilde{\mathbf{b}} \tilde{u}(t) \\ &\leq -\tilde{\lambda} \|\tilde{\mathbf{x}}\|^2 + 2\alpha \hat{\omega}_{max} \sqrt{1 + \tilde{k}^2} \|\tilde{\mathbf{x}}\| |\tilde{u}(t)| \\ &= -(1 - \tilde{\chi}) \tilde{\lambda} \|\tilde{\mathbf{x}}\|^2 - \tilde{\chi} \tilde{\lambda} \|\tilde{\mathbf{x}}\|^2 + 2\alpha \hat{\omega}_{max} \sqrt{1 + \tilde{k}^2} \|\tilde{\mathbf{x}}\| |\tilde{u}(t)| \\ &\leq -(1 - \tilde{\chi}) \tilde{\lambda} \|\tilde{\mathbf{x}}\|^2 \end{aligned} \quad (2.21)$$

for $\tilde{\chi} \in (0, 1)$ and

$$\|\tilde{\mathbf{x}}\| \geq \frac{2\alpha \hat{\omega}_{max} \sqrt{1 + \tilde{k}^2}}{\tilde{\chi} \tilde{\lambda}} |\tilde{u}(t)|. \quad (2.22)$$

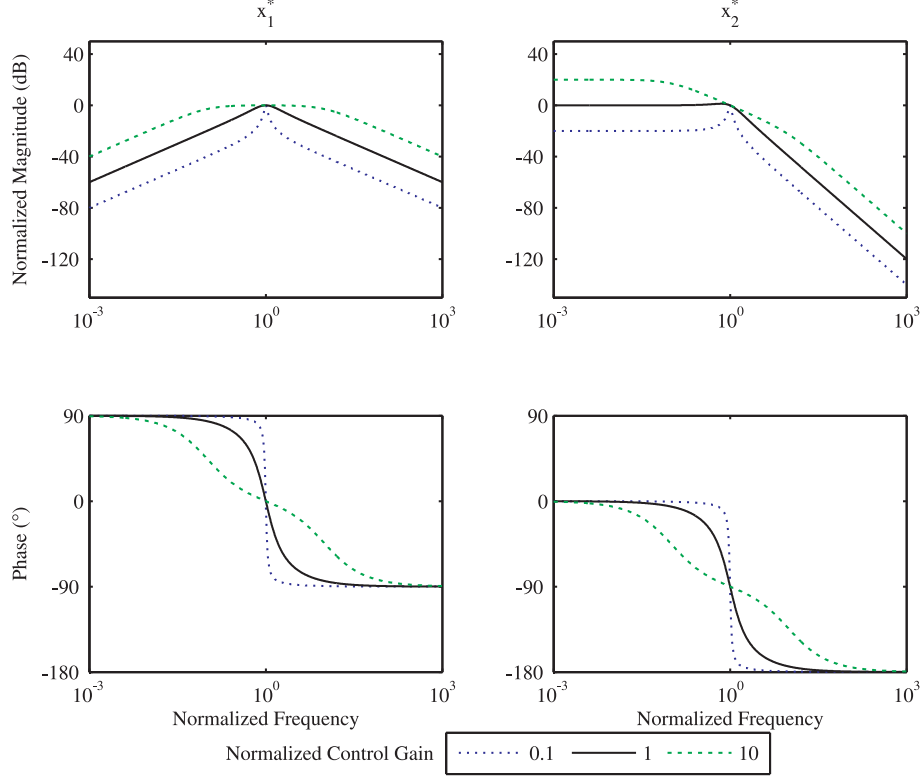


Figure 2.1: Steady-state normalized magnitude and phase of x_1^* and x_2^* . Normalized frequency is $\omega/\hat{\omega}$

Therefore, the input-to-state stability of the trajectory system can be demonstrated (e.g., [32]) with

$$\begin{aligned} \|\tilde{\mathbf{x}}(t)\| &\leq \sqrt{\frac{1+\tilde{k}}{1-\tilde{k}}} \|\tilde{\mathbf{x}}(t_0)\| e^{\frac{-(1-\tilde{\chi})\tilde{\lambda}}{2(1+\tilde{k})}(t-t_0)} \\ &\quad + \sqrt{\frac{1+\tilde{k}}{1-\tilde{k}}} \frac{2\alpha\hat{\omega}_{max}\sqrt{1+\tilde{k}^2}}{\tilde{\chi}\tilde{\lambda}} \sup_{\tau \in [t_0, t]} |\tilde{u}(\tau)|. \end{aligned} \quad (2.23)$$

The input-to-state stability of the trajectory system ensures that the trajectory of the trajectory system $\tilde{\mathbf{x}}(t)$ is bounded for bounded magnitude of the unperturbed input $\tilde{u}(t) = M(t)$, regardless of variations in $\omega(t)$ or $\hat{\omega}(t) \in [\hat{\omega}_{min}, \hat{\omega}_{max}]$. Also, the trajectory of the trajectory system converges to zero if the magnitude of the unperturbed input converges to zero.

2.3 Properties of Trajectory System

The steady-state behavior of the filter can be analyzed by consideration of the trajectory system. In steady state, $\tilde{u}(\cdot) = M(\cdot)$, $\omega(\cdot)$, and $\hat{\omega}(\cdot)$ are constants. Thus, the matrix $\tilde{\mathbf{A}}(\cdot)$ is constant. Without loss of generality, \tilde{u} and ω are assumed to be positive in this section. The steady-state value of $\tilde{\mathbf{x}}$ is given by

$$\tilde{\mathbf{x}} = \tilde{\mathbf{A}}^{-1} \tilde{\mathbf{b}} \tilde{u}. \quad (2.24)$$

Substituting these values into (2.4) and (2.5) reveals that x_1^* and x_2^* are sinusoidal in steady state. In particular, the magnitude of x_i^* is $|x_i^*| = \sqrt{A_i^2 + B_i^2}$ where $i \in \{1, 2\}$, this magnitude is proportional to \tilde{u} , and the normalized magnitude can be expressed as $|x_i^*|/\tilde{u}$. Likewise, the phase of x_i^* with respect to the input u^* is $\angle x_i^* = -\arctan(B_i, A_i)$. Both the magnitude and phase depend on the control parameter α and the normalized frequency $\omega/\hat{\omega}$. The normalized magnitude and phase of x_1^* and x_2^* are shown in Figure 2.1. It can be seen that, when $\hat{\omega} = \omega$, x_1^* is equal to u^* and that x_2^* has the same magnitude as u^* but lags it by 90° .

Solving for the frequencies at which $|x_1^*|/\tilde{u} = 1/\sqrt{2} \approx -3$ dB yields the so called 3-dB bandwidth. It can be shown that the 3-dB bandwidth of the filter is equal to $\alpha\hat{\omega}$, the control gain of the filter. The normalized bandwidth can be expressed as α . A highly selective filter should have a small bandwidth. The settling time of the filter can be determined by the eigenvalues of $\tilde{\mathbf{A}}$. It can be shown that the negative of the maximum real part of any eigenvalue of $\tilde{\mathbf{A}}$, herein labeled the settling rate, is

$$r = - \max_{\lambda \in \text{eig } \tilde{\mathbf{A}}} \Re \lambda = \frac{\alpha\hat{\omega}}{2} - \frac{1}{2} \begin{cases} 0 & \alpha \leq 2 \\ \hat{\omega}\sqrt{\alpha^2 - 4} & \alpha > 2. \end{cases} \quad (2.25)$$

A filter that settles quickly should have a large settling rate. The settling rate can be normalized by $\hat{\omega}$. In Figure 2.2, the normalized bandwidth and normalized settling rate are plotted. It can be seen that there is a trade off between selectivity (low bandwidth) and settling time (high settling rate). For values of $\alpha \leq 2$, increasing

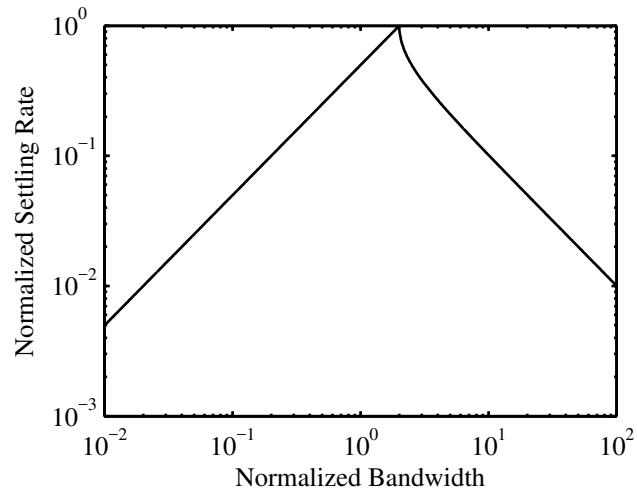


Figure 2.2: Trade off between bandwidth and settling rate.

the bandwidth results in a faster settling time. Increasing the bandwidth beyond 2 actually results in a slower settling rate.

2.4 Generalization to Multiple Frequency Inputs

In many applications, the input to the filter may not be composed of a sinusoid of a single frequency ω . It is possible that harmonics or other spectral content may be present. Although (1.6) is time-varying, it is a linear system. Therefore, superposition can be used to analyze its response when subjected to inputs with multiple frequencies. Suppose

$$u(t) = \sum_{k=1}^K u_k^*(t) + v(t) \quad (2.26)$$

where

$$u_k^*(t) = M_k(t) \cos \theta_k \quad (2.27)$$

$$\dot{\theta}_k = \omega_k \quad (2.28)$$

and $\theta_k(t_0) = \theta_{k0}$ for $k \in \{1, 2, \dots, K\}$. The unperturbed trajectory of the tracking filter can be described as

$$x_1^* = \sum_{k=1}^K x_{1k}^* \quad (2.29)$$

$$x_2^* = \sum_{k=1}^K x_{2k}^* \quad (2.30)$$

where

$$x_{1k}^* = A_{1k} \cos \theta_k + B_{1k} \sin \theta_k \quad (2.31)$$

$$x_{2k}^* = A_{2k} \cos \theta_k + B_{2k} \sin \theta_k \quad (2.32)$$

and where the coefficients of (2.31) and (2.32) evolve according to

$$\dot{\tilde{\mathbf{x}}}_k = \underbrace{\begin{bmatrix} -\alpha & -\omega_k(t) & -\hat{\omega}(t) & 0 \\ \omega_k(t) & -\alpha & 0 & -\hat{\omega}(t) \\ \hat{\omega}(t) & 0 & 0 & -\omega_k(t) \\ 0 & \hat{\omega}(t) & \omega_k(t) & 0 \end{bmatrix}}_{\tilde{\mathbf{A}}_k(t)} \tilde{\mathbf{x}} + \tilde{\mathbf{b}}\tilde{u}_k(t) \quad (2.33)$$

where $\tilde{\mathbf{x}}_k = [A_{1k} \ B_{1k} \ A_{2k} \ B_{2k}]^T$ and $\tilde{u}_k(t) = M_k(t)$. Also, let $\tilde{\mathbf{x}}_k(t_0) = \tilde{\mathbf{x}}_{k0}$ be chosen such that

$$\sum_{k=1}^K \begin{bmatrix} \cos \theta_{k0} & \sin \theta_{k0} & 0 & 0 \\ 0 & 0 & \cos \theta_{k0} & \sin \theta_{k0} \end{bmatrix} \tilde{\mathbf{x}}_{k0} = \mathbf{x}_0. \quad (2.34)$$

By generalizing the analysis to multiple frequency inputs, it is possible to understand the response of the filter by individually considering the response of the filter to each frequency independently. For example, the steady-state response of the filter can be understood by examination of the magnitude and phase response shown in Figure 2.1 for each frequency of input. This approach is used in Section 3.2.

2.5 Dynamics of Unperturbed Filter Trajectory

Having established the unperturbed trajectory of the tracking filter above, it is possible to examine the filter's dynamics about the equilibrium trajectory. Let $\mathbf{z} = \mathbf{x} - \mathbf{x}^*$ where $\mathbf{x}^* = [x_1^* \ x_2^*]^T$. Also, observe that $v(t) = u(t) - u^*(t)$. Then,

$$\dot{\mathbf{z}} = \dot{\mathbf{x}} - \dot{\mathbf{x}}^* = \mathbf{A}(t)\mathbf{z} + \mathbf{b}v(t). \quad (2.35)$$

This error system describes the evolution of the state variable errors with respect to the unperturbed trajectory.

Stability of Error System

The stability of the error system can be understood by consideration of the following Lyapunov function:

$$V(\mathbf{z}) = \mathbf{z}^T \underbrace{\begin{bmatrix} k & 1 \\ 1 & k \end{bmatrix}}_{\mathbf{P}} \mathbf{z} \quad (2.36)$$

where

$$k > \left(\frac{\tilde{\alpha}}{4} + \frac{1}{\tilde{\alpha}} \right) \geq 1 \quad (2.37)$$

for $\tilde{\alpha} > 0$. The positive definiteness of symmetric \mathbf{P} can be assessed through its eigenvalues, which are $k \pm 1$. Each of these is positive for $k > 1$. Therefore, the eigenvalues of symmetric \mathbf{P} are positive, \mathbf{P} is a positive-definite matrix, and $V(\cdot)$ is a positive-definite function. Furthermore,

$$(k - 1)\|\mathbf{z}\|^2 \leq V(\mathbf{z}) \leq (k + 1)\|\mathbf{z}\|^2. \quad (2.38)$$

Let

$$\begin{aligned} \mathbf{Q}(t) &= -(\mathbf{A}^T(t)\mathbf{P} + \mathbf{P}\mathbf{A}(t)) \\ &= \begin{bmatrix} (2\alpha k - 2)\hat{\omega} & \alpha\hat{\omega} \\ \alpha\hat{\omega} & 2\hat{\omega} \end{bmatrix}. \end{aligned} \quad (2.39)$$

The positive definiteness of symmetric $\mathbf{Q}(t)$ can be assessed through its eigenvalues, which are $(\alpha k \pm \sqrt{\alpha^2 k^2 + \alpha^2 - 4\alpha k + 4})\hat{\omega}$. Each of these is positive for $\alpha^2 - 4\alpha k + 4 < 0$. Suppose that $\alpha^2 - 4\alpha k + 4 \geq 0$. Then,

$$\alpha^2 - 4\alpha \left(\frac{\alpha}{4} + \frac{1}{\alpha} \right) + 4 \geq 0 \quad (2.40)$$

$$\alpha^2 - \alpha^2 - 4 + 4 < 0 \quad (2.41)$$

$$0 < 0 \quad (2.42)$$

which is impossible. Therefore, the eigenvalues of symmetric $\mathbf{Q}(t)$ are positive, and $\mathbf{Q}(t)$ is a positive-definite matrix. Further, let

$$\lambda = \max_{\hat{\omega} \in [\hat{\omega}_{min}, \hat{\omega}_{max}]} (\alpha k - \sqrt{\alpha^2 k^2 + \alpha^2 - 4\alpha k + 4})\hat{\omega}. \quad (2.43)$$

The nature of the objective function in (2.43) is such that the maximum occurs at one of the endpoints. From above, $\lambda > 0$ is a lower bound on the eigenvalues of $\mathbf{Q}(t)$ and

$$-\mathbf{z}^T \mathbf{Q}(t) \mathbf{z} \leq -\lambda \|\mathbf{z}\|^2. \quad (2.44)$$

The time derivative of the Lyapunov function is

$$\begin{aligned}
\dot{V} &= (\mathbf{z}^T \mathbf{A}^T(t) + v(t) \mathbf{b}^T) \mathbf{P} \mathbf{z} + \mathbf{z}^T \mathbf{P} (\mathbf{A}(t) \mathbf{z} + \mathbf{b} v(t)) \\
&= -\mathbf{z}^T \mathbf{Q}(t) \mathbf{z} + 2\mathbf{z}^T \mathbf{P} \mathbf{b} v(t) \\
&\leq -\lambda \|\mathbf{z}\|^2 + 2\alpha \hat{\omega} \sqrt{k^2 + 1} \|\mathbf{z}\| |v(t)| \\
&= -(1 - \chi)\lambda \|\mathbf{z}\|^2 - \chi\lambda \|\mathbf{z}\|^2 + 2\alpha \hat{\omega} \sqrt{k^2 + 1} \|\mathbf{z}\| |v(t)| \\
&\leq -(1 - \chi)\lambda \|\mathbf{z}\|^2
\end{aligned} \tag{2.45}$$

for $\chi \in (0, 1)$ and

$$\|\mathbf{z}\| \geq \frac{2\alpha \hat{\omega} \sqrt{k^2 + 1}}{\chi\lambda} |v(t)|. \tag{2.46}$$

Therefore, the input-to-state stability of the perturbed error system can be demonstrated with

$$\begin{aligned}
\|\mathbf{z}(t)\| &\leq \sqrt{\frac{k+1}{k-1}} \|\mathbf{z}(t_0)\| e^{\frac{-(1-\chi)\lambda}{2(k+1)}(t-t_0)} \\
&\quad + \sqrt{\frac{k+1}{k-1}} \frac{2\alpha \hat{\omega} \sqrt{k^2 + 1}}{\chi\lambda} \sup_{\tau \in [t_0, t]} |v(\tau)|.
\end{aligned} \tag{2.47}$$

The input-to-state stability of the error system ensures that the error trajectory $\mathbf{z}(t)$ (the deviation of the filter trajectory $\mathbf{x}(t)$ from the unperturbed trajectory $\mathbf{x}^*(t)$) is bounded for bounded noise $v(t)$, regardless of variations in $\hat{\omega}(t) \in [\hat{\omega}_{min}, \hat{\omega}_{max}]$. Also, the error trajectory converges to zero and the filter trajectory converges to the unperturbed trajectory if the noise converges to zero.

Chapter 3 Proposed Design's Simulation Analysis

In the previous chapter the proposed tracking filter non-linear design has been mathematically analyzed for its stability using Lyapunov's theories. This chapter presents the simulation of the proposed filter and its performance is evaluated.

MATLAB and Simulink software tools are used to model the tracking filter and produce outputs for inputs with harmonic distortion. For this a model of a system that produces harmonics is also designed and the filter's control parameter is selected to provide the most effective results.

The design of the harmonic source and the criteria for the control parameter selection are explained in the following section followed by the comparison of performances of the proposed tracking filter, a basic low pass filter and the reference QSG-SOGI filter.

3.1 Selected harmonic source

A three-phase full-wave diode bridge rectifier is considered in this thesis as a harmonic source to evaluate the performance of the proposed tracking filter. This type of rectifier is extensively used in industry to provide low (>5 kW) to moderately high (<100 kW) dc input power to devices like motor drives or to convert the output of a generator in a power plant for storage in a battery bank.

The disadvantage in using this rectifier is that it has nonlinear characteristics and poor input power factor. The rectifier design used in Simulink to produce the required harmonically distorted power signals is shown below in Figure 3.1.

The three-phase diode rectifier circuit has six diodes connected in a bridge network. When provided with an undistorted three phase input of v_{as} , v_{bs} and v_{cs} to the rectifier, two diodes one each from top and bottom groups conduct at a time. This

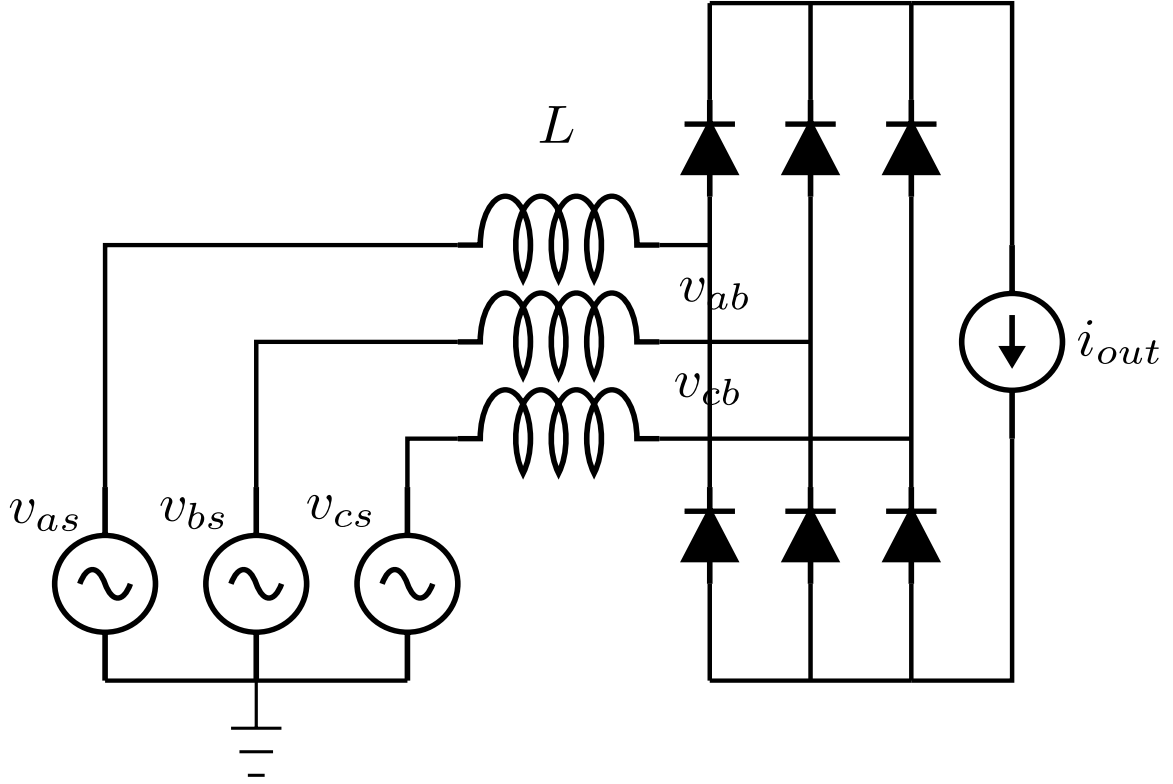


Figure 3.1: Full wave three phase rectifier simulink design

switching of these diodes draws non-sinusoidal current from the input, injecting significant current harmonics [39] into the power network. The grid interface is assumed to be an infinite bus with sinusoidal voltages in series with a reactance. The non-sinusoidal currents drawn by the rectifier will produce non-sinusoidal voltage drops in the series reactance.

Therefore, significant voltage harmonics will be present at the terminals of the rectifier. Many devices like VFDs have rectifiers and the load keeps changing in these devices causing a change in frequency thus creating time varying harmonics in the system.

Thus making a rectifier produced harmonics an useful example to show the tracking capabilities of the proposed filter. In this application, it is required to track the fundamental of the terminal voltages of the rectifier.

3.2 Filter Parameter Selection

Thus far, the only constraint required for stability is that the control gain α is positive. In this section we analyze the requirements of the application and determine the value of α .

The proposed filter's control gain has to be selected so that it provides an optimal output without compromising either THD or settling rate. This can be analyzed and selected by understanding the output characteristics of the filter for various α values for a constant input fundamental frequency. For this purpose the harmonically distorted voltage signals v_{ab} and v_{bc} from the rectifier are used as inputs. To measure the proposed design's performance for its optimal control gain parameter a standard low pass filter is also studied for its output's characteristics for different values of its time constant τ .

The THD, settling rate (*rads/sec*) and the rms phase error (*rad*) is calculated for the outputs of the LPF and the tracking filter. The settling rate and the phase errors are plotted against the corresponding THD values in Figure 3.2. This trade-off will be used to select the control gain for the rectifier application.

The low pass filter's output is processed after the simulation data is collected to compensate for the standard phase error it introduces in its output. This trade off is a multiple objective optimization where neither the THD should be too high for better settling rate nor the settling rate too low for a lower THD. Let us consider a settling rate(*rads/s*) = 60 for this application, the advantage of the proposed filter design is its choice of two α value selections for the same settling rate and both of those α values have their corresponding THD values lower than the standard of 3%. These two points are:

1. $\alpha = 0.31831$
2. $\alpha = 6.433$

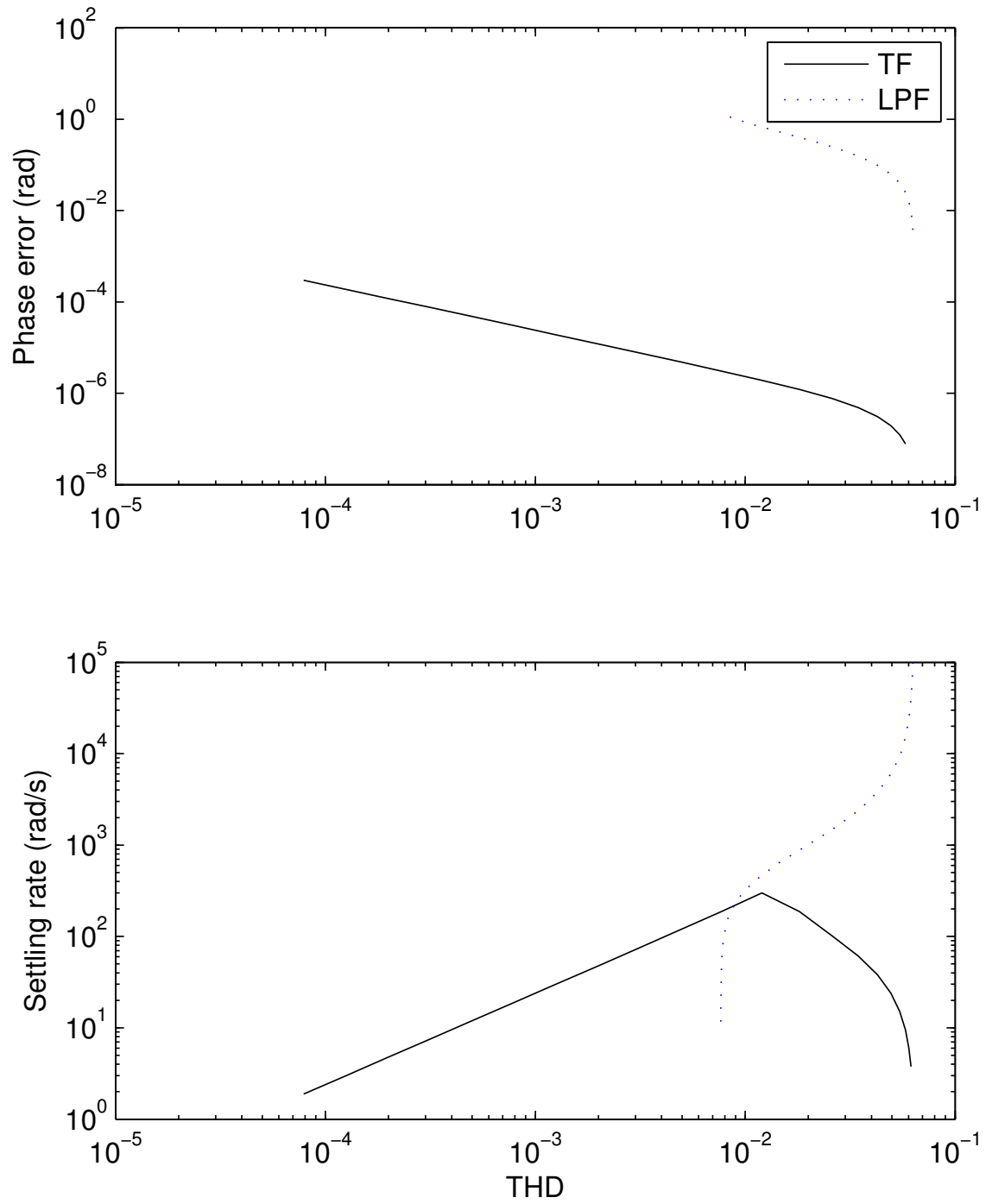


Figure 3.2: Control parameter (α) value selection based on settling rate and Phase error variation with THD variation.

where the trade off for the tracking filter can be seen at the 1st α value with a very low THD and settling rate = 60rads/s . It can also be observed that for the LPF there are two points of interest which are :

1. $\tau = 0.0166s$

2. $\tau = 3.981 \times 10^{-4}s$

These values are used in the following section to show the superiority of the tracking filter's performance for the required trade off.

3.3 Comparison with standard low pass filter

In this section the basic advantage of the proposed tracking filter system which is compactly expressed in 1.6 over a general low pass filter is established.

The simulated harmonic distorted power from the rectifier shown in the Figure 3.3 is filtered using the proposed tracking filter and the low pass filter.

The output of the filters for the 2 sets of control parameters α and τ are plotted for a single cycle. The output of the low pass filter is also amplified as the filtering causes a loss in the magnitude.

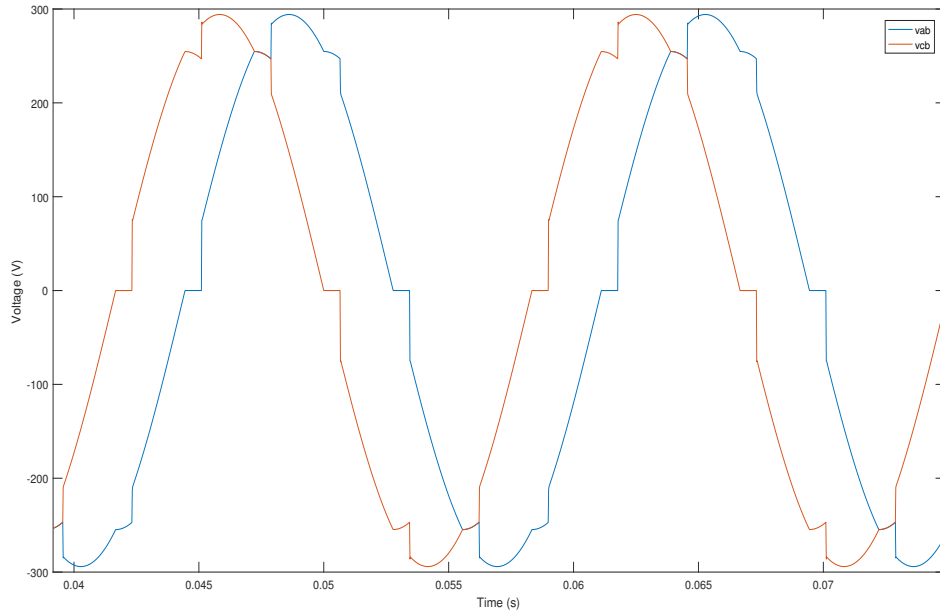


Figure 3.3: Harmonically distorted rectifier input voltages v_{ab} and v_{bc}

First considering settling rate = 60rads/s the required output characteristic of the filter for the rectifier application with the standard THD limit of 3% where $\alpha = 6.433$ and comparing with the LPF's output with nearly the same THD at $\tau = 3.981 \times 10^{-4}\text{s}$.

In Figure 3.4 the undistorted fundamental and the Tracking filter's output are almost overlapping with a very little distortion while the LPF has some distortion as

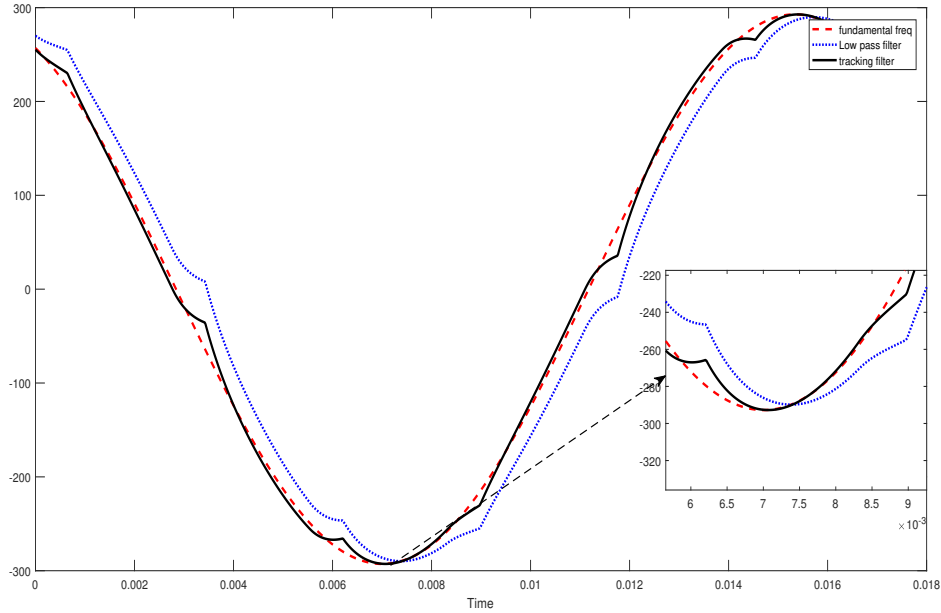


Figure 3.4: Comparison of tracking abilities of the proposed filter and a Low pass filter

well as a visible phase error.

In the Figure 3.5 (a) the output waves frequencies are calculated and plotted along with the undistorted fundamental frequency.

In Figure 3.5(b) the phase errors of both outputs are calculated with the undistorted fundamental as reference. This plot 3.5(b) shows that both the filters have almost equal phase error.

For the of $\alpha = 6.433$ the settling rate and THD obtained in the simulation process are 60.0917rads/sec and 3.53% respectively while for $\tau = 3.981 \times 10^{-4}\text{s}$ these values are 2511.9rads/s and 3.56% respectively.

In this above measured values it can be observed that though the THD limit is met by both the filters and the low pass filter having higher settling rate the phase error for both is high which is not desirable in tracking power signals.

Moving to the lower phase error region of the Figure 3.2 there is an $\alpha = 0.31831$ which satisfies the settling rate condition of 60rads/s and taking the point where the

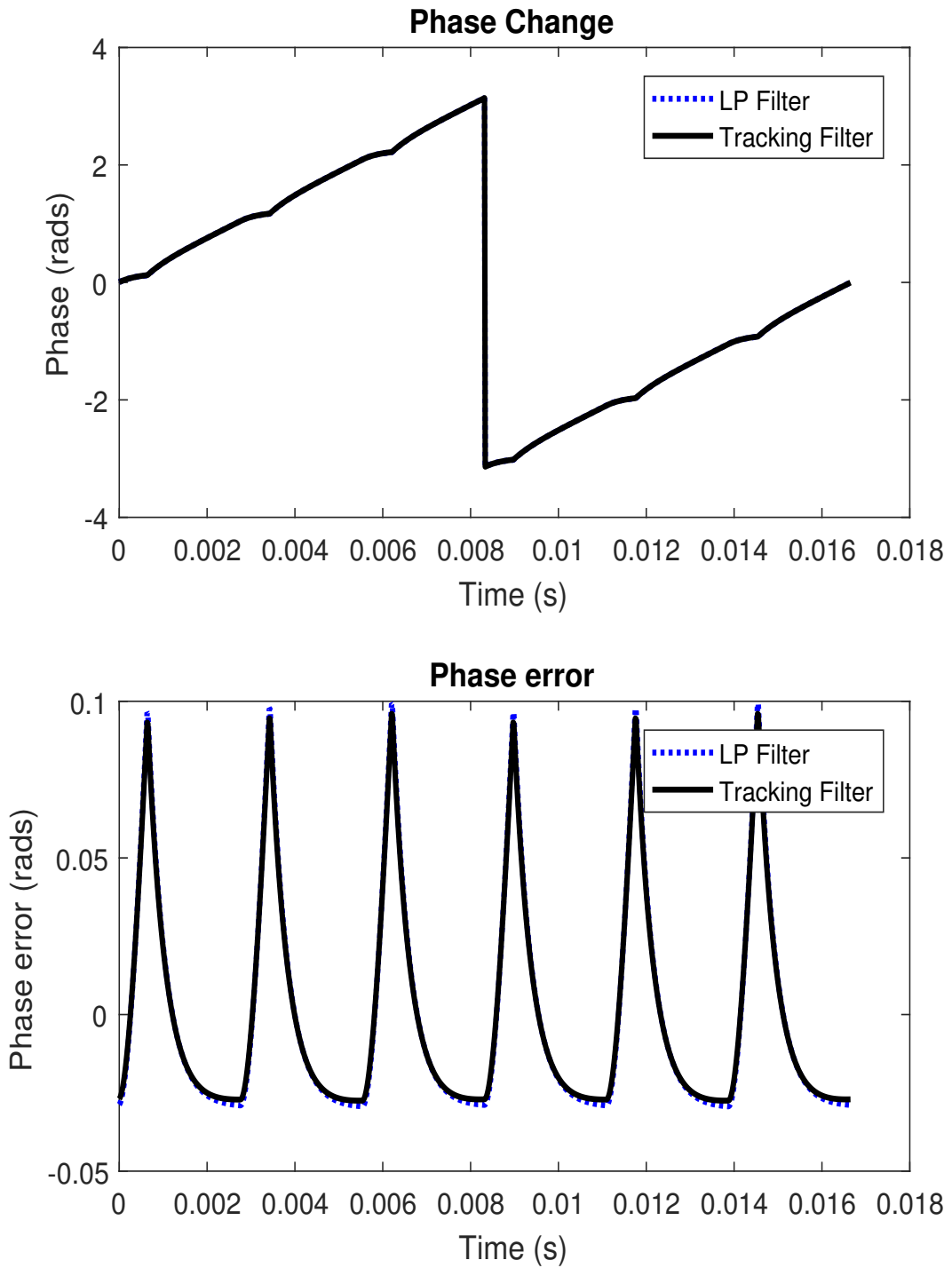


Figure 3.5: Phase change and phase error comparison for α & τ at THD = 3%

LPF also satisfies the same requirement at $\tau = 0.0166s$. These two parameters are used and their outputs are plotted similar to the above case in Figure 3.6.

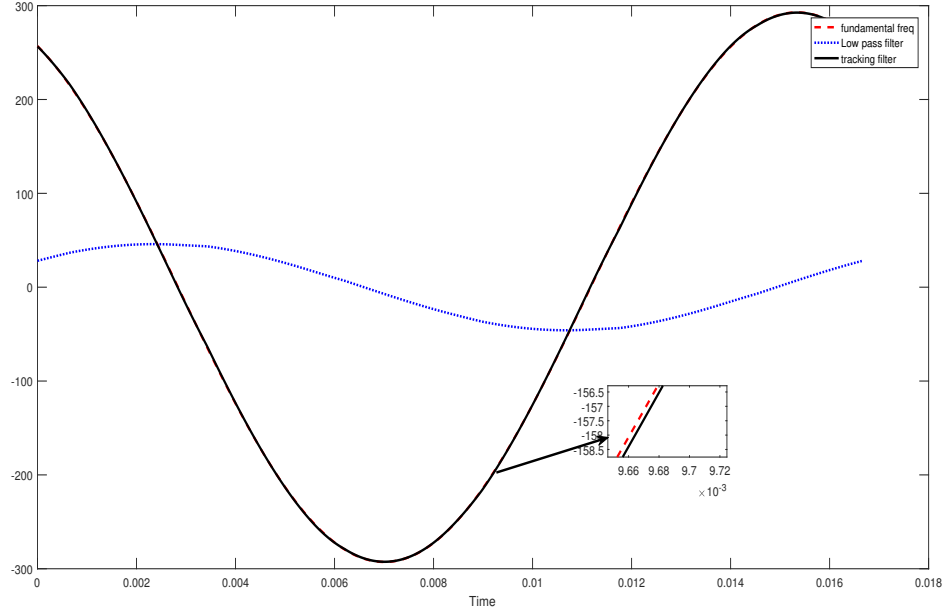


Figure 3.6: Output comparison of TF & LPF for α & τ at Settling Rate = 60 rads/s

In Figure 3.7 we can observe that the proposed tracking filter output is overlapping the fundamental signal while the LPF's output is attenuated. Though from Figure 3.2 its can be observed that the phase error of both the filters are nearly the same the phase change and phase error for these points they are plotted in Figure 3.7 for a clearer understanding of the error.

Both filter's output characteristics are calculated while the settling rate remains a constant $60rads/s$. The THD values for the tracking filter and LPF are 0.0025 and 0.0077 respectively. Though the errors are nearly equal the output of the tracking filter is comparatively more accurate than that of LPF.

This simulation results show the proposed tracking filter's has an advantage over LPF due to its design which provides a better trade off in the multiple value optimization issue of THD and settling rate.

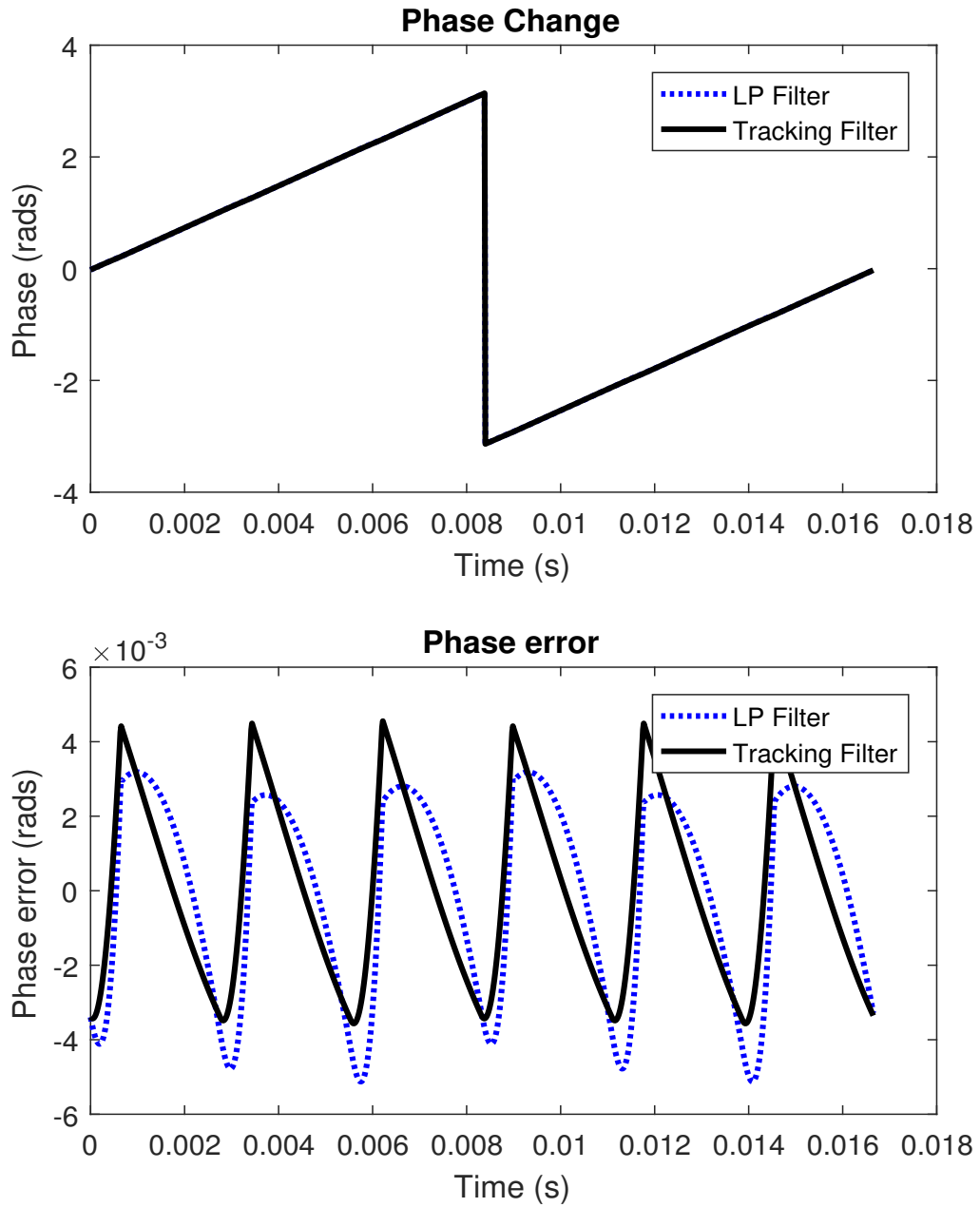


Figure 3.7: Phase change and phase error comparison for α & τ at settling rate = 60rads/sec

This gives the tracking filter design a clear superiority over the basic methods of harmonic filtering.

Copyright© Pranav Aramane, 2018.

3.4 Variable Frequency Harmonic Distortion Filtering Performance

The proposed Tracking Filter is proved to provide good results when the fundamental frequency is not time varying in the last section. To show that it outperformed the existing novel Second Order Generalized Integrator based Quadrature Signal Generator (SOGI-QSG) 3.1, they are both tested in a time varying fundamental frequency simulation.

$$\begin{bmatrix} \dot{x}_1 \\ \dot{x}_2 \end{bmatrix} = \begin{bmatrix} -\alpha\hat{\omega}(t) & -\hat{\omega}^2(t) \\ 1 & 0 \end{bmatrix} \begin{bmatrix} x_1 \\ x_2 \end{bmatrix} + \begin{bmatrix} \alpha\hat{\omega}(t) \\ 0 \end{bmatrix} u(t) \quad (3.1)$$

Simulation Results

The results of the simulation explained above are discussed here.

To demonstrate this improvement in the design a ramp is applied to the fundamental which also affects its 3rd and 9th harmonics. This distorted fundamental frequency is filtered simultaneously using the proposed and the QSG-SOGI filters.

In the Figure 3.8(a) the output of both the filters are plotted along with the undistorted fundamental. It can be observed in this plot that the QSG-SOGI does not lock on the changed fundamental frequency as well as the designed filter.

In Figure 3.8(b) the error of the outputs for each filter are calculated by subtracting them from the fundamental and are plotted. This shows that the error of the proposed tracking filter is lower than the QSG-SOGI. It can also be observed that the QSG-SOGI's error spikes during the transition where as the proposed filter's stays low. The proposed design's error if analyzed, lowers quicker than the QSG-SOGI - showing better settling rate.

To demonstrate better, zoomed in scope outputs are shown below:

The Figure 3.9 shows the transition phase where the frequency fluctuates rapidly around time period of 1.5 s where the error standard deviation is 0.0155 for tracking

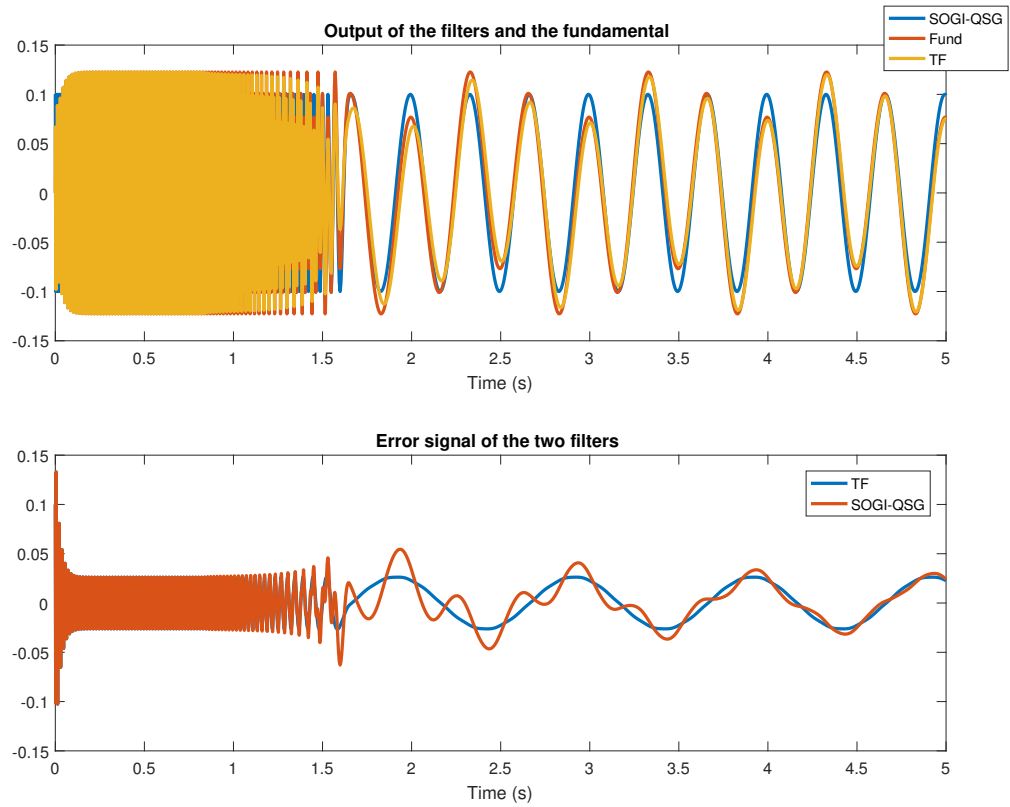


Figure 3.8: (a) Filtered Output (b) Error signals of both filters - in variable frequency conditions

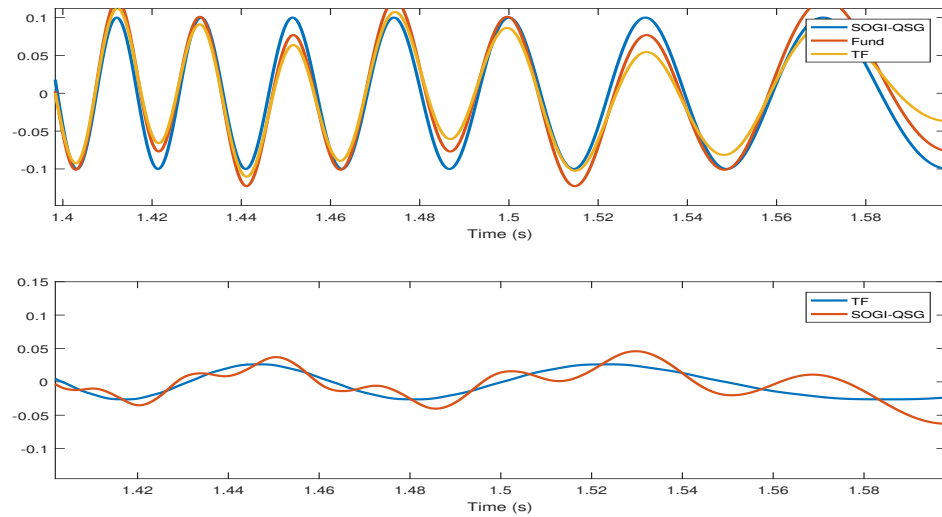


Figure 3.9: Zoomed in plot during the rapid frequency change

filter and 0.0196 for the QSG-SOGI.

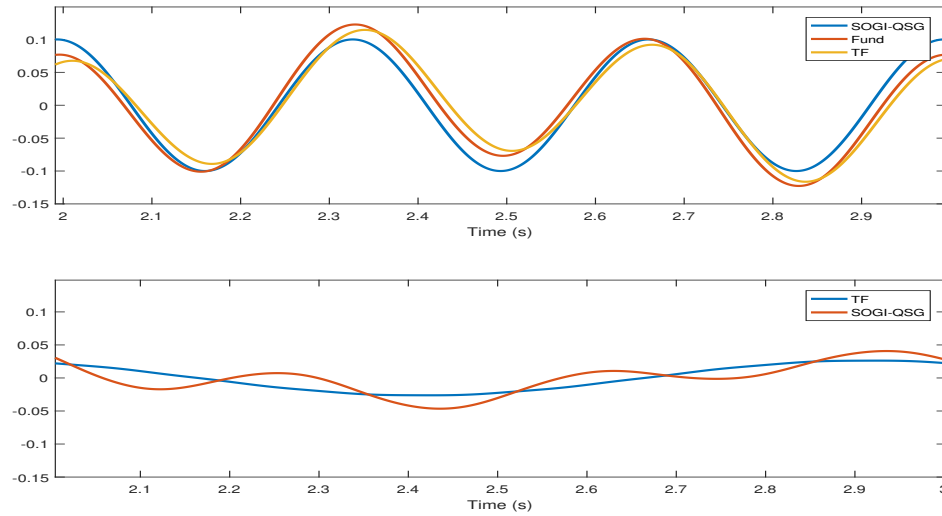


Figure 3.10: Zoomed in plot immediately after rapid frequency change

The Figure 3.10 shows the phase where the frequency fluctuation slows down and the tracking filter output almost overlaps with the fundamental around time period of 2.5 s. Here the tracking filter error standard deviation is 0.0108 while it is 0.0132 for the novel filter.

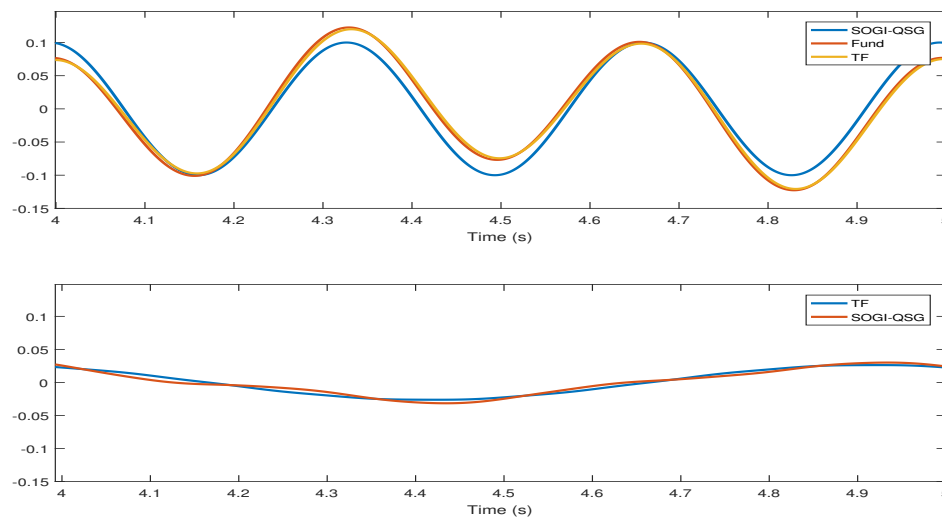


Figure 3.11: Zoomed in plot with settled output of TF

The Figure 3.11 shows where tracking filter output is settled with negligible error. Even though SOGI-QSG's error standard deviation is as low as that of the tracking filter around 0.0084 it is still fluctuating more than the proposed filter's error.

These results demonstrate the main advantage of the proposed tracking filter over the QSG-SOGI as is its quick frequency tracking in rapid frequency varying conditions.

Chapter 4 Conclusion

Tracking and filtering of harmful harmonics is crucial for maintaining good quality of power. The increase of harmonic sources like non linear devices, transformers, generators, arc flash equipment on both load and generation sides is making this a critical problem. There are already many existing techniques like using line reactors and passive and active filter designs like RC & Kalman filters to mitigate harmonics. In addition to mitigating the known disturbances it is also important to estimate and measure them to maintain the power quality. This will ensure that if the harmonics are in the prescribed standard limits there will be no negative impacts like damage to electrical equipment and false operation of essential devices thus reducing the economic losses.

Summary of Contribution

1. This thesis has proposed a filter that can accurately track the fundamental and reject fast varying harmonics. The proposed filter is an improved version of the design recently proposed for detecting line-to-ground faults in high resistance ground networks [31]. It is designed to be more dependent on frequency to increase its tracking abilities.
2. The non linear filter design stability has been analyzed by using the Lyapunov theory. Mathematical analysis determined its unperturbed filter trajectory and its stability. It has sound input-to-state stability and the trade off between settling rate and bandwidth is mathematically determined to select the control parameter. The filter is also proved to have an error system with bounded input-to-state stability and its trajectory converges to zero when generalized for multiple inputs.

3. MATLAB/Simulink tools were used to model the tracking filter and produce filtered output signals from inputs with harmonic distortions. A three-phase full-wave diode bridge rectifier was used as the harmonic source. The harmonics induced input due to the switching of the diodes is ideally suited to evaluate the tracking filter. To demonstrate the tracking filter's performance a basic low pass filter was also modeled and simulated with the same input. Its fast tracking ability is displayed in comparison to a modeled novel SOGI-QSG filter for a harmonically distorted rapid frequency varying input.
4. When compared with the Low pass filter for a fundamental with constant frequency for a desired settling rate, the total harmonic distortion (THD) was 0.0025 for an alpha value of 0.31831. Though the corresponding THD value for the low pass filter was only little more than double that of the proposed tracking filter, there was a significant difference in the output signals generated by the low pass and tracking filters. While there was high attenuation in the output generated by the low pass filter, the output generated by the proposed tracking filter was almost identical when compared to the fundamental.
5. The results are presented for the simulations of the proposed and novel SOGI-QSG filters for fast varying frequency tracking. The clear advantage of the tracking filter is shown in terms of its better settling rates. The tracking filter was able to settle quicker after the transient period of frequency change as well as the error during the change was less when compared with the SOGI-QSG filter. This is due to its design with increased frequency dependency than the filter it is based on.

This filter can be used to estimate fundamental or a particular harmonic to directly compensate for it and reduce the distortion.

Future Work

In this thesis an existing design was improved analyzed and simulated however, there is still room for improvement.

1. There can be more design improvements to reduce the error in tracking and have better trade off for the desired settling rate.
2. Simulink designed full wave rectifier signals were used to test the stability and performance. The design should be tested with other simulated sources to establish its performance before implementation.
3. Frequency variation testing can be further improved by filtering stored real time data from grid or power supply distress conditions.
4. Actual implementation and real time testing of this proposed design can be done for applications with rapid frequency variations to track the fundamental accurately like in VFDs and UPS.

Bibliography

- [1] V. Kumar, A. S. Pandey, and S. K. Sinha, “Grid integration and power quality issues of wind and solar energy system: A review,” in *2016 International Conference on Emerging Trends in Electrical Electronics Sustainable Energy Systems (ICETEESES)*, March 2016, pp. 71–80.
- [2] “Short-Term Energy Outlook - U.S. Energy Information Administration (EIA),” https://www.eia.gov/outlooks/steo/report/renew_co2.php, (Accessed on 03/05/2018).
- [3] S. Khan, B. Singh, and P. Makhija, “A review on power quality problems and its improvement techniques,” in *2017 Innovations in Power and Advanced Computing Technologies (i-PACT)*, April 2017, pp. 1–7.
- [4] H. D. Mathur, “Enhancement of power system quality using distributed generation,” in *2010 IEEE International Conference on Power and Energy*, Nov 2010, pp. 567–572.
- [5] V. Khadkikar, R. K. Varma, R. Seethapathy, A. Chandra, and H. Zeineldin, “Impact of distributed generation penetration on grid current harmonics considering non-linear loads,” in *2012 3rd IEEE International Symposium on Power Electronics for Distributed Generation Systems (PEDG)*, June 2012, pp. 608–614.
- [6] F. Blaabjerg, R. Teodorescu, M. Liserre, and A. V. Timbus, “Overview of control and grid synchronization for distributed power generation systems,” *IEEE Transactions on Industrial Electronics*, vol. 53, no. 5, pp. 1398–1409, Oct 2006.
- [7] N. Anandh, P. A. D’sa, M. V. Gautam, and V. S. Sandeep, “Power quality estimation, analysis and improvement for uninterrupted power supply,” in *2016 In-*

- ternational Conference on Control, Instrumentation, Communication and Computational Technologies (ICCICCT)*, Dec 2016, pp. 26–31.
- [8] C.-S. Li, Z.-X. Bai, X.-Y. Xiao, Y.-M. Liu, and Y. Zhang, “Research of harmonic distortion power for harmonic source detection,” in *2016 17th International Conference on Harmonics and Quality of Power (ICHQP)*, Oct 2016, pp. 126–129.
- [9] A. Symonds and M. Laylabadi, “Cycloconverter drives in mining applications: A typical industrial system is analyzed and the impact of harmonic filtering considered,” *IEEE Industry Applications Magazine*, vol. 21, no. 6, pp. 36–46, Nov 2015.
- [10] G. W. Chang, Y. J. Liu, H. M. Huang, and S. Y. Chu, “Harmonic analysis of the industrial power system with an ac electric arc furnace,” in *2006 IEEE Power Engineering Society General Meeting*, 2006, pp. 4 pp.–.
- [11] A. Subramaniam, A. Sahoo, S. S. Manohar, and S. K. Panda, “Voltage and current-harmonics induced ageing in electrical insulation,” in *2017 International Symposium on Electrical Insulating Materials (ISEIM)*, Sept 2017, pp. 403–406.
- [12] P. M. Nicolae, M. . Nicolae, I. D. Smrndescu, and I. D. Nicolae, “Concerns on electromagnetic compatibility and power quality issues at a three-phase transformer,” in *2017 IEEE International Symposium on Electromagnetic Compatibility Signal/Power Integrity (EMCSI)*, Aug 2017, pp. 377–382.
- [13] V. E. Wagner, J. C. Balda, D. C. Griffith, A. McEachern, T. M. Barnes, D. P. Hartmann, D. J. Phileggi, A. E. Emmanuel, W. F. Horton, W. E. Reid, R. J. Ferraro, and W. T. Jewell, “Effects of harmonics on equipment,” *IEEE Transactions on Power Delivery*, vol. 8, no. 2, pp. 672–680, Apr 1993.

- [14] L. Cividino, "Power factor, harmonic distortion; causes, effects and considerations," in *Telecommunications Energy Conference, 1992. INTELEC '92., 14th International*, Oct 1992, pp. 506–513.
- [15] N. Eghtedarpour, M. A. Karimi, and M. Tavakoli, "Harmonic resonance in power systems - a documented case," in *2014 16th International Conference on Harmonics and Quality of Power (ICHQP)*, May 2014, pp. 857–861.
- [16] P. B. Petrovi, "Power harmonics estimation based on analytical signal concept," in *2017 International Symposium on Power Electronics (Ee)*, Oct 2017, pp. 1–6.
- [17] J. Zhang, H. Wen, L. Tang, Z. Teng, and Z. Chen, "Frequency shifting and filtering algorithm for power system harmonic estimation," in *2017 IEEE International Workshop on Applied Measurements for Power Systems (AMPS)*, Sept 2017, pp. 1–6.
- [18] J. Sun, S. Ye, and E. Aboutanios, "Robust and rapid estimation of the parameters of harmonic signals in three phase power systems," in *2016 24th European Signal Processing Conference (EUSIPCO)*, Aug 2016, pp. 408–412.
- [19] "Ieee recommended practice and requirements for harmonic control in electric power systems - redline," *IEEE Std 519-2014 (Revision of IEEE Std 519-1992) - Redline*, pp. 1–213, June 2014.
- [20] A. Timbus, M. Liserre, R. Teodorescu, P. Rodriguez, and F. Blaabjerg, "Evaluation of current controllers for distributed power generation systems," *IEEE Transactions on Power Electronics*, vol. 24, no. 3, pp. 654–664, March 2009.
- [21] S. Lewis, V. Nuo, E. Barocio, P. Zuiga, and F. A. Uribe, "Dynamic tracking of power system harmonics with a new kalman-wavelet technique," in *2015 IEEE International Autumn Meeting on Power, Electronics and Computing (ROPEC)*, Nov 2015, pp. 1–6.

- [22] L. Motta and N. Fandes, "Active / passive harmonic filters: Applications, challenges trends," in *2016 17th International Conference on Harmonics and Quality of Power (ICHQP)*, Oct 2016, pp. 657–662.
- [23] D. Schwanz, A. Bagheri, M. Bollen, and A. Larsson, "Active harmonic filters: Control techniques review," in *2016 17th International Conference on Harmonics and Quality of Power (ICHQP)*, Oct 2016, pp. 36–41.
- [24] M. Khan, N. Salman, A. Ali, A. Khan, and A. Kemp, "A comparative study of target tracking with kalman filter, extended kalman filter and particle filter using received signal strength measurements," in *Emerging Technologies (ICET), 2015 International Conference on*. IEEE, 2015, pp. 1–6.
- [25] T. Xu, Q. Ge, X. Feng, and C. Wen, "Strong tracking filter with bandwidth constraint for sensor networks," in *Control and Automation (ICCA), 2010 8th IEEE International Conference on*. IEEE, 2010, pp. 596–601.
- [26] K. Nishi, S. Ando, and S. Aida, "Optimum harmonics tracking filter for auditory scene analysis," in *Acoustics, Speech, and Signal Processing, 1996. ICASSP-96. Conference Proceedings., 1996 IEEE International Conference on*, vol. 1. IEEE, 1996, pp. 573–576.
- [27] S.-K. Chung, "A phase tracking system for three phase utility interface inverters," *Power Electronics, IEEE Transactions on*, vol. 15, no. 3, pp. 431–438, 2000.
- [28] K. Sun, Q. Zhou, and Y. Liu, "A phase locked loop-based approach to real-time modal analysis on synchrophasor measurements," *Smart Grid, IEEE Transactions on*, vol. 5, no. 1, pp. 260–269, 2014.

- [29] T. Kwan and K. Martin, “Adaptive detection and enhancement of multiple sinusoids using a cascade IIR filter,” *Circuits and Systems, IEEE Transactions on*, vol. 36, no. 7, pp. 937–947, 1989.
- [30] B. C. Neagu, G. Grigora, and F. Scarlatache, “The influence of harmonics on power losses in urban distribution networks,” in *2016 International Symposium on Fundamentals of Electrical Engineering (ISFEE)*, June 2016, pp. 1–4.
- [31] C. D. Rodríguez-Valdez and R. J. Kerkman, “Method to detect line-to-ground faults in high-resistance-ground networks,” in *Energy Conversion Congress and Exposition (ECCE), 2010 IEEE*. IEEE, 2010, pp. 2284–2292.
- [32] H. Khalil, *Nonlinear Systems*. Prentice Hall, 2000. [Online]. Available: https://books.google.com/books?id=v_BjPQAACAAJ
- [33] Z. Xin, C. Yoon, R. Zhao, P. C. Loh, and F. Blaabjerg, “Realization of quadrature signal generator using accurate magnitude integrator,” in *2016 IEEE Energy Conversion Congress and Exposition (ECCE)*, Sept 2016, pp. 1–8.
- [34] T. Q. Tho, T. V. Anh, and L. M. Phuong, “Estimation of voltage parameters for grid-connected inverters,” in *2015 International Conference on Advanced Technologies for Communications (ATC)*, Oct 2015, pp. 610–615.
- [35] M. S. Reza, M. Ciobotaru, and V. G. Agelidis, “Frequency adaptive instantaneous power quality analysis using frequency locked loop based kalman filter technique,” in *2012 3rd IEEE International Symposium on Power Electronics for Distributed Generation Systems (PEDG)*, June 2012, pp. 767–774.
- [36] F. Antunes, L. S. Xavier, A. F. Cupertino, L. B. Felix, and H. A. Pereira, “Comparison of harmonic detection methods applied in a photovoltaic inverter during harmonic current compensation,” in *2017 Brazilian Power Electronics Conference (COBEP)*, Nov 2017, pp. 1–6.

- [37] S. Golestan, S. Y. Mousazadeh, J. M. Guerrero, and J. C. Vasquez, “A critical examination of frequency-fixed second-order generalized integrator-based phase-locked loops,” *IEEE Transactions on Power Electronics*, vol. 32, no. 9, pp. 6666–6672, Sept 2017.
- [38] M. Xie, C. Zhu, Y. Yang, and H. Wen, “Srf-pll with in-loop differentiator decouple filter for unbalanced three-phase systems,” in *2017 IEEE Applied Power Electronics Conference and Exposition (APEC)*, March 2017, pp. 1314–1318.
- [39] M. McCarty, A. Pratama, M. Anwari *et al.*, “Harmonic analysis of input current of single-phase controlled bridge rectifier,” in *2009 IEEE Symposium on Industrial Electronics and Applications*, 2009, p. 520.

Vita

Pranav Aramane

Education

B.E. in Electronics and Communication Engineering May 2013

Vasavi College of Engineering

Osmania University, Hyderabad, India

Experience

SCADA Engineer December 2016 - Present

Siemens Gamesa Renewable Energy, Trevose, PA

SCADA Intern July 2016 - December 2016

Siemens Gamesa Renewable Energy, Trevose, PA

SCADA Intern June 2014 - August 2014

EDPR N.A., Houston, TX